

<h1>DNMI - RAPPORT</h1> <p>NORWEGIAN METEOROLOGICAL INSTITUTE BOX 43 BLINDERN , N - 0313 OSLO</p> <p>PHONE +47 22 96 30 00</p>	ISSN 0805-9918
	REPORT NO. 24/00 KLIMA
	DATE 22.12.00
TITLE Temperature scenarios for Norway Empirical downscaling from the ECHAM4/OPYC3 GSDIO integration	
AUTHORS <p style="text-align: center;">I. Hanssen-Bauer, O.E. Tveito and E.J. Førland</p>	
PROJECT CONTRACTORS Norwegian Research Council (Contract no 120656/720) and Norwegian Meteorological institute.	
<p><u>Abstract</u></p> <p>The 2m temperature field from the ECHAM4/OPYC3 GSDIO integration (which includes effects of greenhouse-gases and tropospheric ozon, as well as direct and indirect effects of sulphur aerosols) was used as predictor for empirical downscaling of local monthly mean temperature over Norway during the period 1870-2050. The reason for using temperature as the only predictor, without including the SLP-field or other circulation indices, is that previous investigations have shown that the observed relations between large-scale SLP-field and temperature is very well reproduced by the ECHAM4/OPYC3 model.</p> <p>The empirically downscaled temperature series indicate average annual warming rates of 0.2 to 0.5 °C per decade up to year 2050 at the Norwegian mainland, and 0.6 °C per decade on Svalbard. The warming rates are generally smallest in southern Norway along the west coast. They increase when moving inland and northwards. At the west coast in southern Norway, the modelled warming rates are rather similar in all seasons (0.2-0.3 °C per decade). Further north and in the inland, considerably larger warming rates are expected in winter than in summer. In Northern Norway and in inland valleys also in Southern Norway, winter warming rates of more than 0.5 °C per decade can be expected. At the Arctic stations the modelled winter warming rates are of magnitude 1 °C per decade.</p> <p>The present results were compared to the results from dynamical downscaling. The results were rather similar in summer and autumn. In winter and spring, on the other hand, systematic differences were found: While the results were still quite similar at the west-coast of Southern Norway, the empirical downscaling gave larger warming rates in the inland, especially in valleys and other locations which are exposed for temperature inversions during winter. It is probably reasonable to expect larger winter warming in valleys than on mountains: The winter warming is probably accompanied by increased cyclonic activity, which leads to less favourable conditions for temperature inversions. Thus the empirical downscaling results may qualitatively be right on this point.</p> <p>Most of the differences between the warming rates calculated from empirical vs. dynamical downscaling results were within the 95% confidence interval for the warming rates.</p>	
SIGNATURE	
..... Eirik Førland Principal Investigator, RegClim-PT3 Bjørn Aune Head of the Climatology Division

Temperature scenarios for Norway

Empirical downscaling from the ECHAM4/OPYC3 GSDIO integration

I. Hanssen-Bauer, O.E. Tveito and E.J. Førland

1. Introduction	5
2. Method and data	7
2.1 Predictands and predictors	7
2.2 Method	10
3. Results	13
3.1 Evaluation based upon the period 1870-2000	13
3.2 Time series 1900-2050 for selected stations	19
3.3 Warming rates – definitions	27
3.4 The warming from 1961-1990 to 2020-2049	30
3.5 Scenarios for derivative characteristics	35
4. Comparisons between empirical and dynamical downscaling	36
5. Summary	43
References	44
Appendix-1, Basic information about stations	46
Appendix-2, Averages and standard deviations of observed and modelled monthly mean temperatures during different 30-year periods at selected stations	47
Appendix-3, Warming rate scenarios (seasonal and annual) for the individual stations ...	53

1. Introduction

One of the overall aims of the RegClim project (Iversen et al. 1997) is to estimate probable changes in the climate in Norway, including Svalbard, under global warming. Coupled atmospheric-ocean global general circulation models (AOGCMs) are the most sophisticated tools for modelling global warming. The resolution in the recent AOGCMs is probably sufficient for modelling large-scale features, but in general still too coarse to enable these models to reproduce the climate on regional or local scale. It is thus a need for downscaling of the results from the AOGCMs.

Within the RegClim project, we have approached this problem both applying dynamical and empirical downscaling techniques (e.g. Murphy 1999). In both tasks, we have mainly been working with the results from the Max-Planck-Institute's AOGCM, ECHAM4/OPYC3 (Roeckner et al., 1996, 1998, 1999), and mainly with the "GSDIO" integration which is a transient integration including greenhouse gases, tropospheric ozone, and direct as well as indirect sulphur aerosol forcing (Roeckner et al. 1999). Results from the dynamical downscaling experiments were reported by Bjørge et al. (2000). In the present report, temperature scenarios from empirical downscaling of the GSDIO integration will be presented and compared to the results from the dynamical downscaling.

The quality of future climate scenarios based upon AOGCMs highly depend on the models' ability to realistically reproduce the large-scale fields of meteorological variables. Improved scenarios on a regional or local scale may be achieved by downscaling techniques only if the large-scale fields that are used as predictors or boundary conditions are realistic. It is thus crucial to validate the large-scale fields produced by the AOGCM integrations against observations (Wilby et al 1999). Benestad et al. (1999) validated monthly fields from the ECHAM4/OPYC3 "present-day climate" simulation with focus on Scandinavia. They noted that the average north-south sea level pressure (SLP) gradient over this area at average is too weak in the model. Christensen et al. (1998) nested the ECHAM4/OPYC3 present-day climate into very high-resolution climate models over Scandinavia, and found a close agreement between modelled and observed temperature climatology except in certain areas in the north with few observations. Hanssen-Bauer and Førland (2000b) validated the ECHAM4/OPYC3 GSDIO integration, which is used as a basis of the present work, over Norway and Svalbard. They concluded that, also in this integration, the north-south SLP gradient over Norway and Svalbard is at average too weak, but the anomalies from the average are realistic. The average monthly temperature fields were found to be fairly realistic, wherever it was possible to find stations reasonably close to the grid points, with similar altitude and distance from coast. It was also concluded that the ECHAM4/OPYC3 mainly is able to reproduce the observed links between the SLP anomalies and the

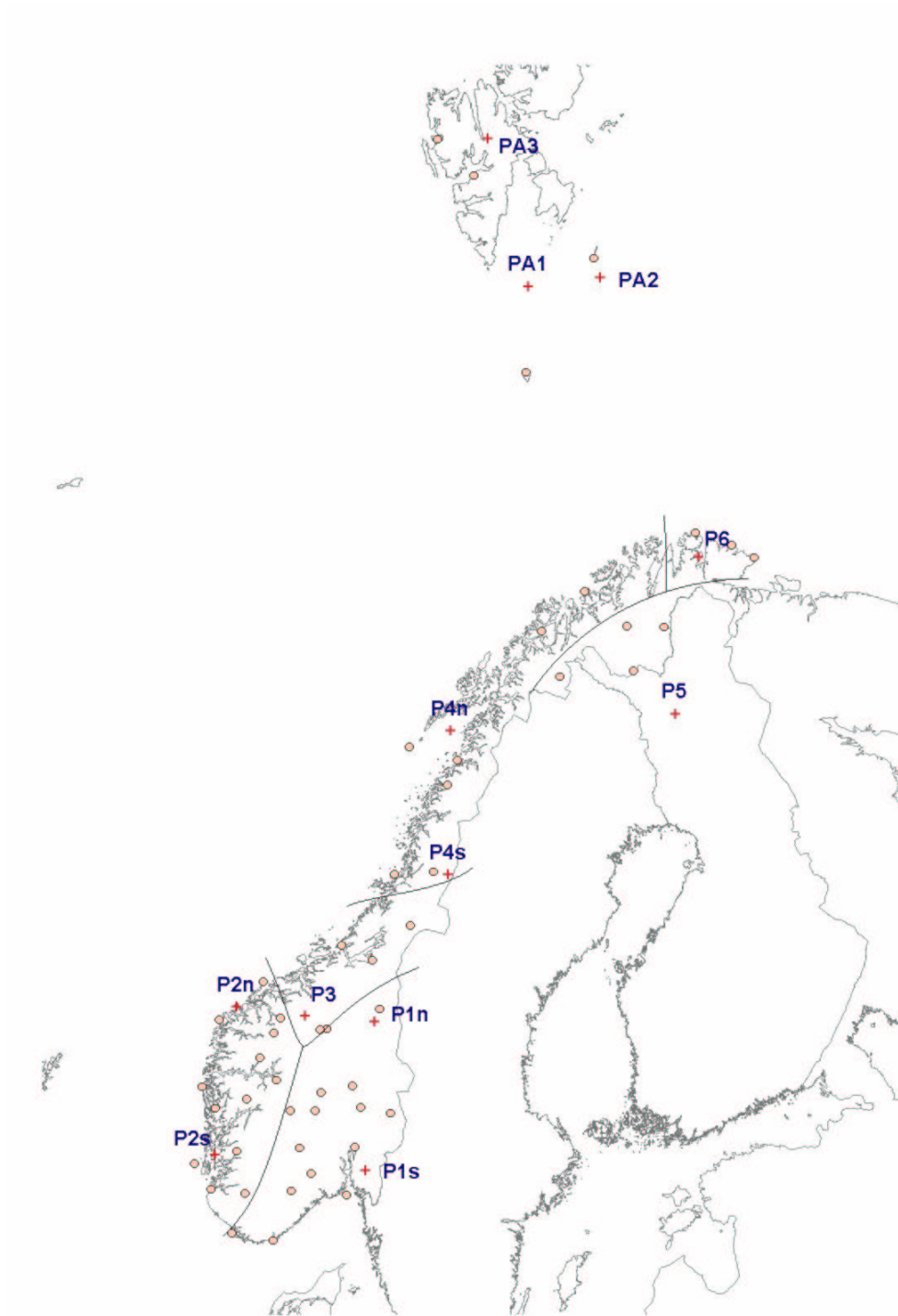


Figure 1. Temperature regions, grid-points and stations used in the present paper.

temperatures in the area, especially in winter when these connections are most pronounced.

The present work is thus based upon a global model integration which reproduces the historical average large-scale temperature over the actual area field fairly well. There is a bias in the average SLP field, however the variation around the average is realistic.

2. Methods and data

“Empirical downscaling” denotes methods involving the use of empirical links between large-scale fields and local variables to deduce estimates of the local variables from the large-scale fields.

Numerous techniques exist for establishing such links (e.g. Zorita and von Storch 1999), including both linear (multivariate regression, singular vector decomposition, canonical correlation) and non-linear ones (analogue techniques, weather classes, neural networks). The optimal choice of method depends highly on the choices of predictors (large-scale input variables), predictands (the local output variables) and the time resolution. E.g., linear techniques are often highly skilled for downscaling temperature, while they may be less good for precipitation, at least on a daily basis.

2.1 Predictands and predictors

In the present work, the predictand is local monthly mean temperature at selected Norwegian stations (Fig. 1). Hanssen-Bauer and Nordli (1998) concluded that the temperature variation at the Norwegian mainland during the last 100 years is described fairly well by standardized monthly series from 6 “temperature regions”, which are characterized by high correlation between temperature observations from different stations within the region. Bjørnøya and Svalbard should probably be defined as two different regions. For the present purpose, it is however convenient to include both in an “Arctic region”, denoted by “A”. Figure 1 shows that all regions are represented by several stations. Table A1 (Appendix) gives geographical coordinates and other relevant information for all stations.

The optimal choice of predictors is dependent on the predictands, but also on the specific problem. When applied for making local climate scenarios from AOGCM global warming scenarios, at least 3 conditions should be fulfilled:

1. The large-scale fields which are used as predictors should be realistically modelled by the AOGCM;
2. The links between the predictors and the local predictands should be strong and robust, i.e. the predictors should account for a dominant part of the variance in the predictands, and the link should be stable in time;
3. At least one of the predictors should carry the “global warming signal”.

A commonly used predictor for downscaling local climate is the SLP-field. This is partly because there exist long global series of gridded SLP, but also because the AOGCMs generally reproduce the main features of the SLP field reasonably well (cf. point 1 above). Hanssen-Bauer and Førland (2000b) showed that the average SLP field from the ECHAM4/OPYC3 GSDIO integration has a bias over Norway. However, as the anomalies from the average field are fairly realistic, one might adjust for this bias, simply by using the anomaly field as predictor rather than the field itself.

Another reason for the outspread use of the SLP field in downscaling studies is that investigations from several locations have shown that it is possible to find robust empirical links between SLP fields and local temperature and/or precipitation, at least during winter (e.g. Werner and von Storch 1993, Zorita et al. 1995, Hanssen-Bauer and Førland 1998) (cf. point 2 above). Hanssen-Bauer and Førland (2000a) demonstrated that condition 2 above to a large degree is satisfied when using large-scale SLP as predictor for local temperature and precipitation in Norway. However, even though the SLP based downscaling models account for a major part of the variance in the local temperatures, the models only partly account for the observed temperature *trends* during the last century. This indicates that some of the warming which occurred in Norway during this period was not connected to changes in the SLP field alone, at least not in a linear way.

Analyses of historical data thus indicate that the warming in Norway during the 20th century was partly, but probably not entirely connected to changes in the atmospheric circulation. When considering the expected future global warming, this is certainly not entirely connected to changes in the atmospheric circulation. The changes in the greenhouse effect may affect the atmospheric circulation, which again will affect the temperature conditions at different locations, but the initial change is connected to the radiative transfer through the atmosphere, which in the first run affects temperature, not SLP. Thus, using the SLP field as the only predictor for local temperature would certainly not satisfy the third of the above conditions. Candidate predictors satisfying point 3 are large-scale thickness fields and temperature fields.

In the present study, we have chosen to use the large scale 2 m temperature field over Norway and Svalbard as predictor for local temperatures. This variable certainly satisfies the last two of the above

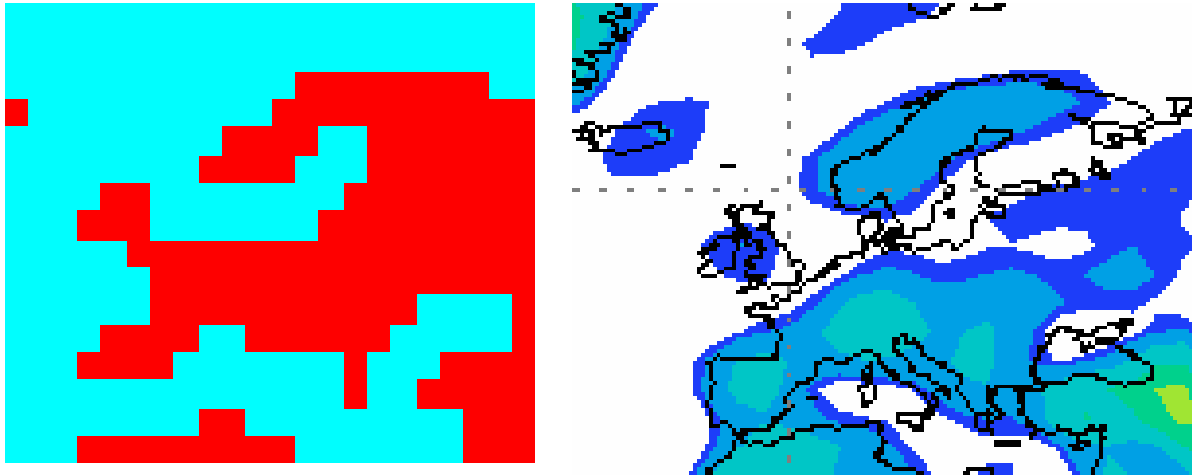


Figure 2. Land-mask (left) and topography (right) for the ECHAM4/OPYC3 GSDIO integration.

conditions, and Hanssen-Bauer and Fjørland (2000b) concluded that the large scale temperature field also is quite realistically modelled by the ECHAM4/OPYC3 over Norway and Svalbard. The first idea was to use both SLP field and 2 m temperature-field as predictors, but as Hanssen-Bauer and Fjørland (2000b) found that ECHAM4/OPYC3 actually reproduces the observed empirical links between SLP field and temperatures quite well, it was concluded that it is sufficient to use the large-scale temperature field as the only predictor.

A problem when using the AOGCM gridded temperature field as predictor is that there are no decisive conclusions of whether grid-point temperatures preferably should be compared to area-averaged observations or directly to local values (Huth et al. 2000, Skelly & Henderson-Sellers 1996). Benestad et al. (1999) concluded that the ECHAM4/OPYC3 monthly averaged grid-point temperatures, at least for continental sites, are closer to station values than to the gridded temperature data from the University of East Anglia, both concerning mean values and standard deviations. Hanssen-Bauer and Fjørland (2000b) concluded that wherever it is possible to find stations and grid-points within the same temperature region with similar altitude and distance from coast, the grid-point values agreed reasonably well with station values. But they also concluded that the standardised grid-point temperature series agreed very well with the standardised regional series, which are actually the average of 3-12 standardised series from stations within a specific region. It is thus concluded that grid-point values could be interpreted as point values, where the point's altitude and continentality are defined by the model topography (which indeed is very different from the real one, cf. Fig. 2). But in standardised form, the series from the grid-point could also be interpreted as regional series representative for the region the grid-point belongs to. The temperature grid-points that are used as predictors in the present downscaling are shown in Figure 1.

2.2 Method

Hanssen-Bauer and Nordli (1998) showed that the monthly temperature series, $T_{,xm}$ for any location (x) within a temperature region (m) in Norway can be estimated by the equation:

$$T_{,xm}(t) \approx ST_m(t) \cdot \sigma_{xm} + \mu_{xm} \quad (1).$$

Here t is time, ST_m is the standardised monthly temperature series for region m , while μ_{xm} and σ_{xm} are mean value and standard deviation for monthly mean temperature at the location x . As stated above, the standardised grid-point temperature series from the ECHAM4/OPYC3 GSDIO integration can be interpreted as a standardised regional series, i.e.:

$$ST_m(t) \approx [T_{pm}(t) - \mu_{pm}] / \sigma_{pm} \quad (2),$$

where T_{pm} is the monthly temperature series for gridpoint p in region m , while μ_{pm} and σ_{pm} are mean value and standard deviation for the monthly mean temperature at this gridpoint.

One may thus define estimates for local temperature series just by combining these equations:

$$\langle T_{xm}(t) \rangle_{est} = [T_{pm}(t) - \mu_{pm}] \cdot (\sigma_{xm} / \sigma_{pm}) + \mu_{xm} \quad (3).$$

When using this equation for downscaling model scenarios, one also have to decide how to define comparable mean values and standard deviations based on observations and model data. One should consider the risk of choosing a period which, within the natural variability of the system, happens to be e.g. unusually cold in the model and unusually warm in reality. Hanssen-Bauer and Nordli (1998) used 1961-1990 as reference period when defining the regional series. The first idea was to use the same period in the downscaling model. Comparisons of different 30-year temperature means showed that these values are reasonably stable, at least up to 1990, both for observations and for model data. For temperature averages, the period 1961-90 is thus a reasonable choice. This is also convenient, as this is the latest standard normal period, for which monthly averages have been published for all Norwegian stations (Aune 1993). For standard deviations, however, 30 year seems to be too short period for getting stable values. Hanssen-Bauer (2000) showed that the standard deviations for the GSDIO monthly grid-point temperatures for different 30-year periods vary rather much. Specifically, the standard deviations for January in some grid-points were considerably lower for the period 1961-1990 than for the periods 1871-1900, 1901-1930 and 1931-1960 (Fig.5 in Hanssen-Bauer 2000), while

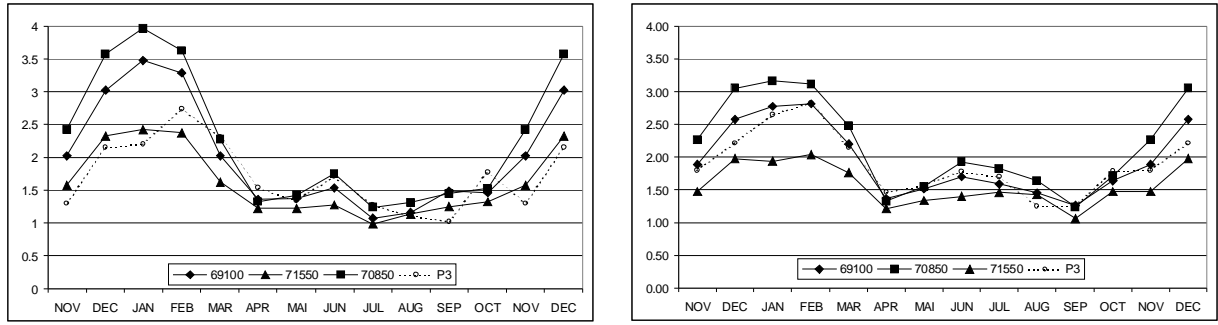


Figure 3. Standard deviation for monthly mean temperature at stations and grid-point in region 3. Left: Based upon the period 1961-1990. Right: Based upon the period 1901-1990

rather the opposite is the case for observations (Fig. 3). It was thus decided that standard deviations for the period 1901-1990 should be used in the downscaling equation (3). For the grid-points, monthly values from the GSDIO integration are available for the period 1860-2050, but only a limited number of stations have data from the entire period 1901-1990. Investigations showed, however, that for stations (e.g. x and y) within the same region (m) and for a given month (i), the ratios between the standard deviations for the period 1901-1990 and 1961-1990 (or any other specific period) were almost identical:

$$\sigma_{xmi}(1901-1990)/\sigma_{xmi}(1961-1990) \approx \sigma_{ymi}(1901-1990)/\sigma_{ymi}(1961-1990) = a_{mi} \quad (4).$$

As there, within every region, is at least one station with measurements during the entire 90-year period, it is thus possible to make estimates for the 90-year standard deviations at a station z within the same region, simply by applying the ratios from stations with long series:

$$\sigma_{zmi}(1901-1990) \approx a_{mi} \cdot \sigma_{zmi}(1961-1990) \quad (5).$$

When using the 90-year period, the correspondence between model grid-points and station values was generally better than for the 30-year period both concerning the absolute values of the standard deviations and concerning the inter-monthly variation. Figure 3 shows the results from grid-point and stations within temperature region 3.

Using the 90-year period for calculating standard deviations, creates some problems in northern Norway. Hanssen-Bauer and Førland (2000b) found that the GSDIO integration includes 2 winters (1931-32 and 1932-33) with unrealistically low temperatures in grid-points near the northern coast of Norway. Figure 4 shows the January temperature anomalies from grid-point 6, and the similar observed anomalies from the near-by station 98550 Vardø. The two outliers affect the standard deviation for the grid-point very much, and in order to avoid this, we chose to regard the periods December through March 1931/32 and 1932/33 as missing in the model data.

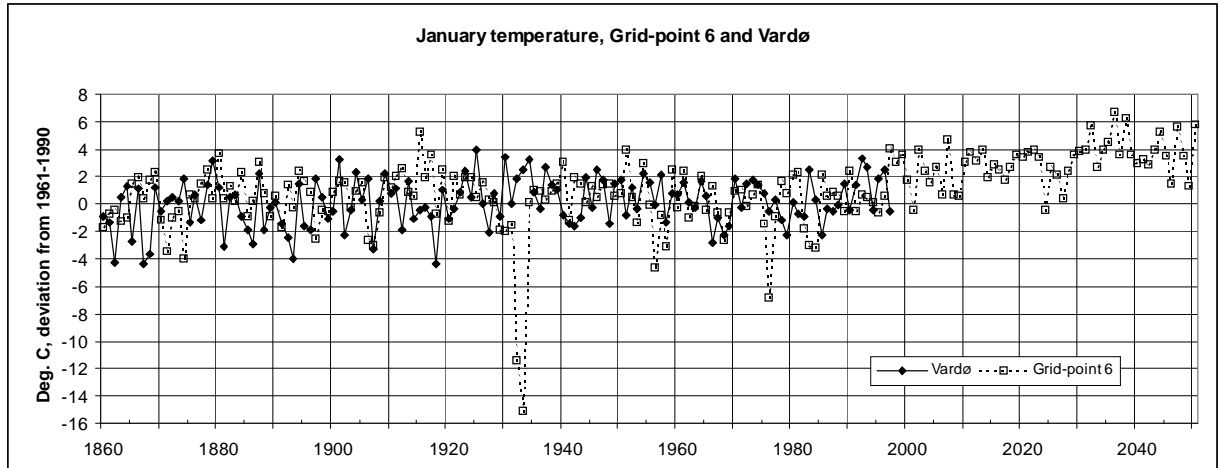


Figure 4. January temperatures in Vardø (observed) and in grid-point 6 (from the GSDIO integration). Both are given as anomalies from the 1961-1990 average.

The implications of this are:

1. The months December through March 1931/32 and 1932/33 are left out when statistical properties (e.g. average and standard deviation) are calculated for periods involving these months. This is done not only for model data, but also for observations in order to get comparable values.
2. When comparing time series of downscaled and observed temperatures (chapter 3), the period December 1931 – March 1932 is replaced by repeating values from the previous year, while values from the succeeding year are applied for the period December 1932 – March 1933.

With these restrictions, the downscaling model can then be expressed in the following way:

$$\langle T_{xm}(t) \rangle_{est} = [T_{pm}(t) - \mu_{pm}(1961-90)] \cdot [\sigma_{xm}(1901-90) / \sigma_{pm}(1901-90)] + \mu_{xm}(1961-90) \quad (6).$$

But rather than calculating the ratio $[\sigma_{xm}(1901-90) / \sigma_{pm}(1901-90)]$ month by month, which still might give some random variation, it was decided to calculate an average “winter-value” which was used for December, January and February, and a “summer value”, which was used for the months April through September. For March, October and November, ratios were chosen between the summer- and winter values.

One might argue that, for consistence, the period 1901-90 should be used also for defining mean values. However, this does only affect the absolute level of the temperature series, not relative values like inter-annual variability, decadal variations and warming rates. Thus the scenarios for local warming are not affected by this.

3. Results

3.1 Evaluation based upon the period 1870-2000

The results from the empirical downscaling of temperature may to a certain degree be evaluated by comparing model data from the period 1870 to 2000 to observations from selected stations. The comparison cannot be done on a year-to-year basis, as natural inter-annual variability is certainly not in phase in model and reality. It is thus the statistical properties that should be compared. In the present report, this is done in two ways. First, observed and modelled standard deviations and averages of monthly mean temperatures over different 30-year periods at selected stations are compared. Secondly, observed and modelled frequency distributions of annual and seasonal mean temperatures over different 50-year periods at selected stations are compared.

Figure 5 shows averages and standard deviations of monthly mean temperatures at 4 stations, while results from other stations with reasonably long temperature series are given in Table A2 in Appendix. Modelled and observed mean values for the period 1961-1990 are identical because this period was used as a reference for modelling temperature changes (see eq. 6). By comparing these values to values from other periods one may, however, get an impression of how realistic the model is. Concerning standard deviations, the period 1901-1990 was used for scaling the model. The average levels of the standard deviations are thus necessarily quite realistic, but again, one may validate the differences between the standard deviations during different 30-year periods. The main impression is that the model in most cases shows realistic variation in the 30-year mean values and standard deviations of monthly mean temperature. However, at some stations, the model standard deviation in the spring and/or autumn months tend to be somewhat larger than observed. This is possible because the ratio between observed and modelled standard deviations were not calculated directly on a monthly basis (cf. eq. 6 and the following paragraph). In spring and autumn they were rather interpolated between typical winter- and summer-values. Getting too high standard deviations in spring thus reflect that the global model overestimates the standard deviation in spring compared to the other seasons.

Figures 6 – 9 show observed and modelled frequency distributions of annual and seasonal mean temperature at 4 stations for different 50-year periods. The differences between the periods 1900-49 and 1950-99 concerning temperature distributions seem to be random (both in model and reality), and they are thus probably caused by natural variability rather than by the difference in radiative forcing. The observed and modelled distributions are in most cases rather similar, though at some locations (e.g. Bergen, Figure 7), the modelled distributions in spring and/or autumn have heavier tails than the observed ones.



Figure 5. Modelled and observed averages and standard deviations of monthly mean temperatures during different 30-year periods at selected stations: Period 0 is 1871-1900, 1 is 1901-1930, 2 is 1931-1960 and 3 is 1961-1990. At stations that started later than 1871, the first period goes from observations started.

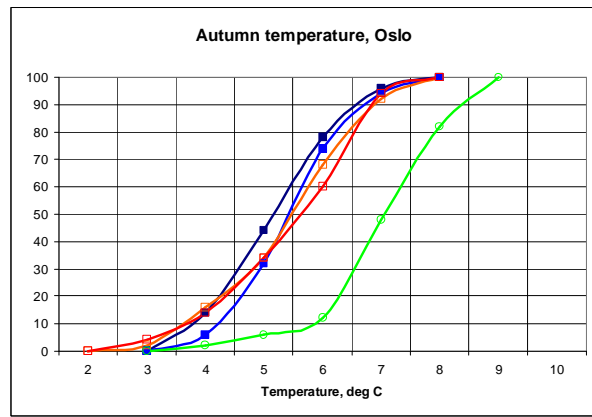
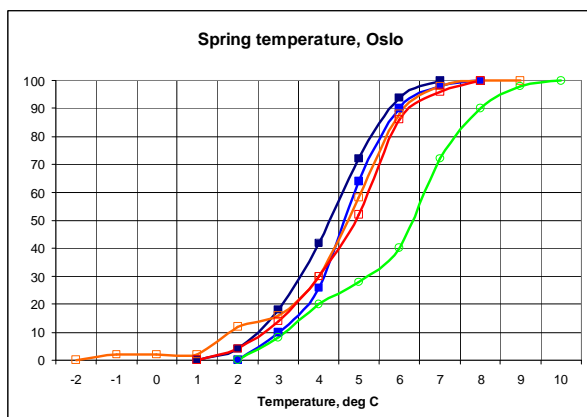
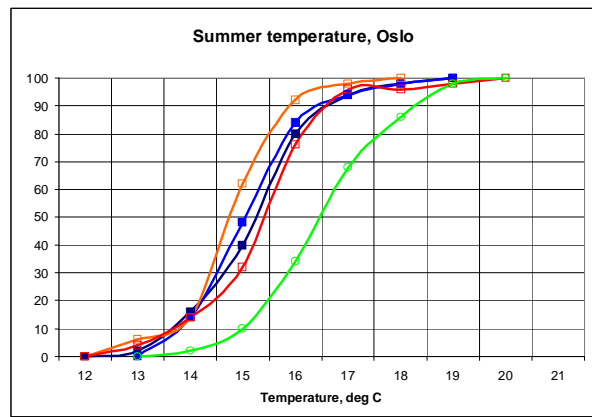
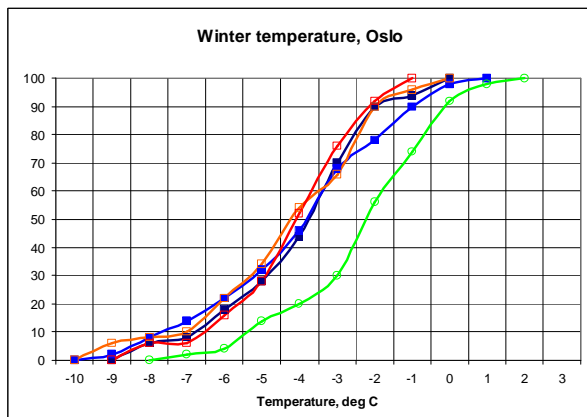
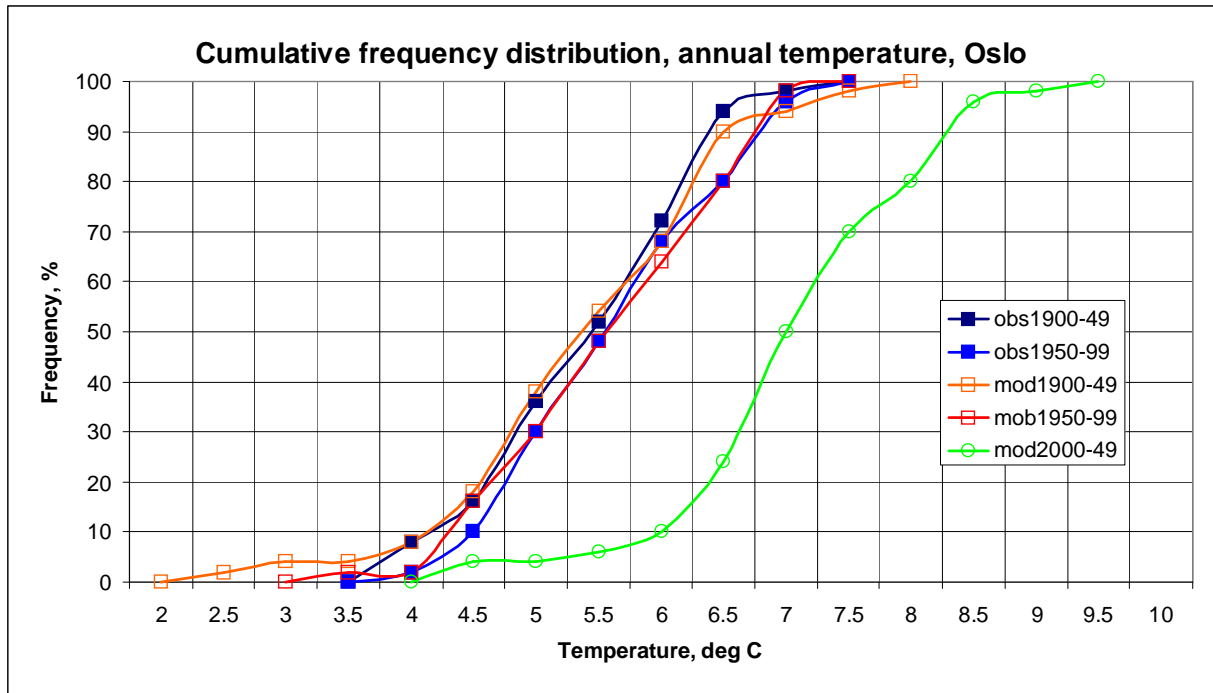


Figure 6. Cumulative frequency distributions of annual and seasonal mean temperatures in Oslo. Blue and red curves show observed and modelled distributions, respectively, based upon the periods 1900-49 and 1950-99. Green curves show modelled distributions for the period 2000-2049.

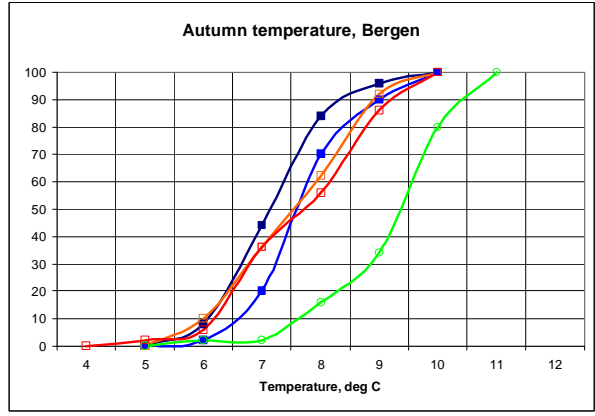
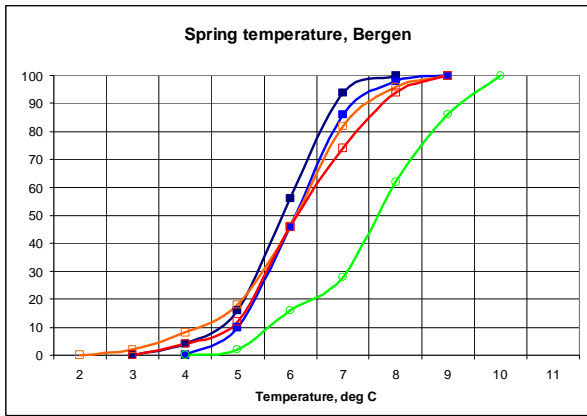
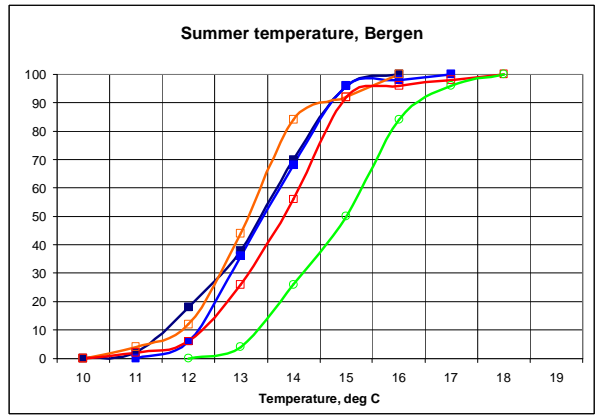
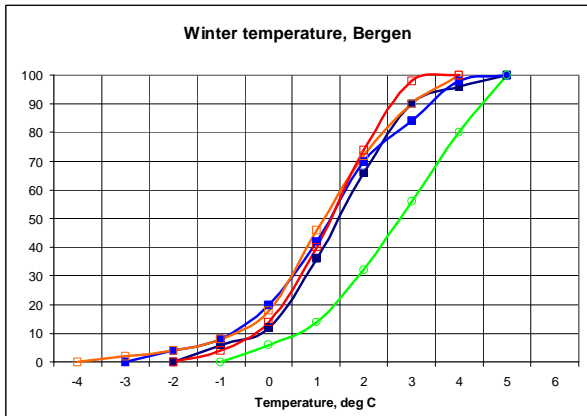
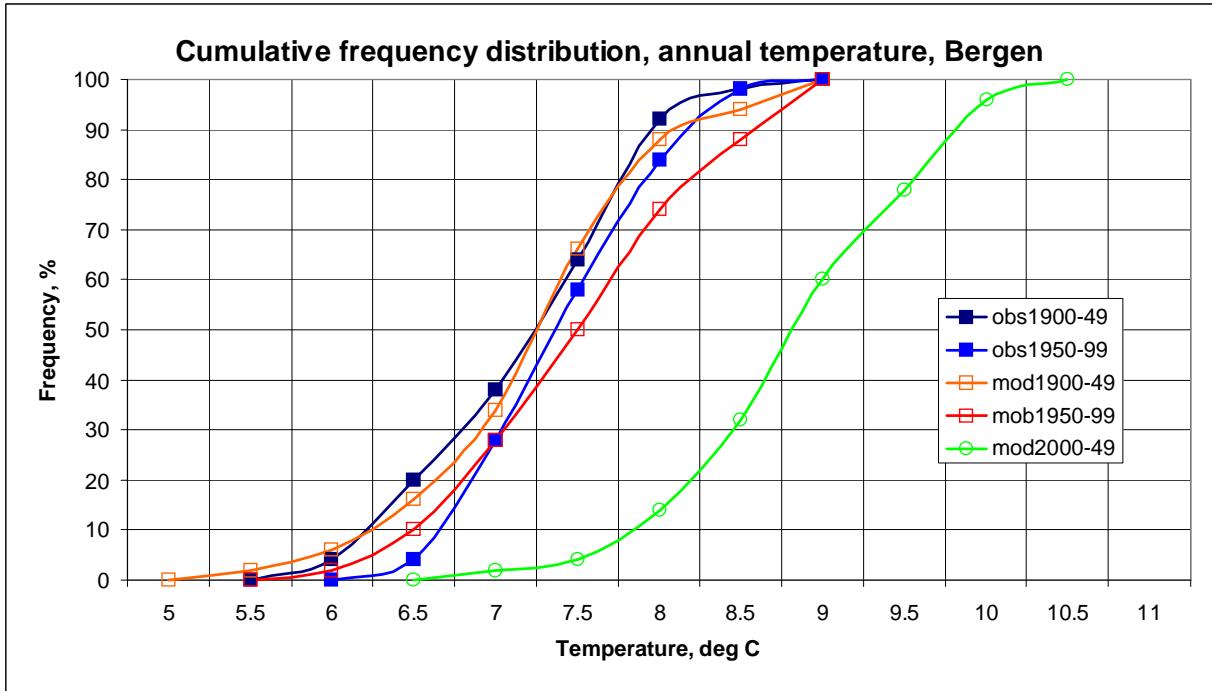


Figure 7. Cumulative frequency distributions of annual and seasonal mean temperatures in Bergen. Blue and red curves show observed and modelled distributions, respectively, based upon the periods 1900-49 and 1950-99. Green curves show modelled distributions for the period 2000-2049.

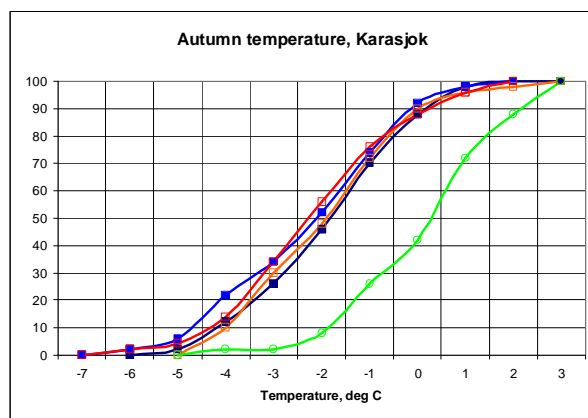
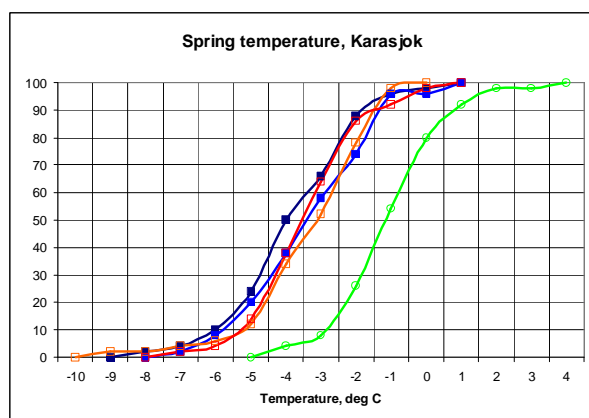
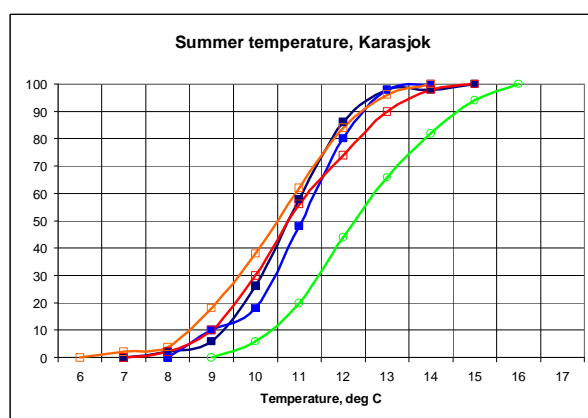
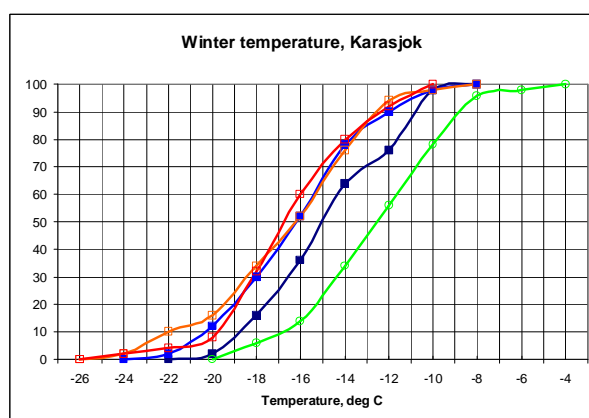
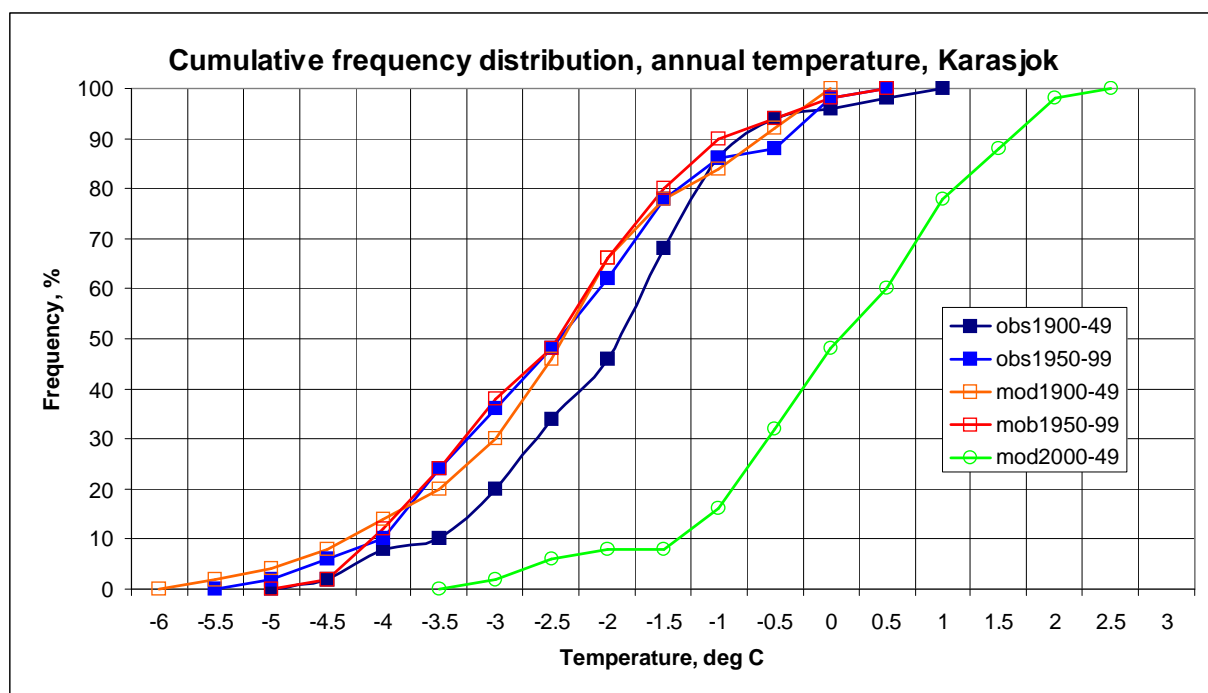


Figure 8. Cumulative frequency distributions of annual and seasonal mean temperatures in Karasjok. Blue and red curves show observed and modelled distributions, respectively, based upon the periods 1900-49 and 1950-99. Green curves show modelled distributions for the period 2000-2049.

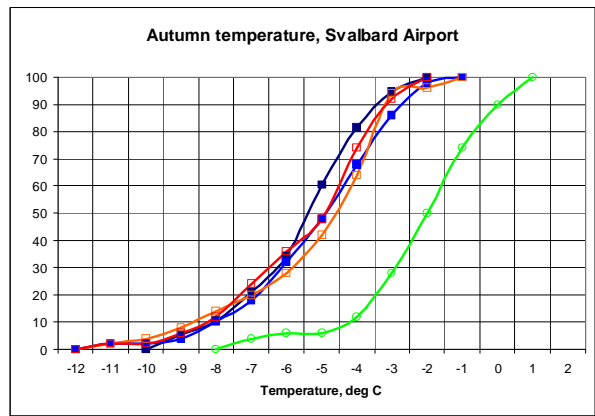
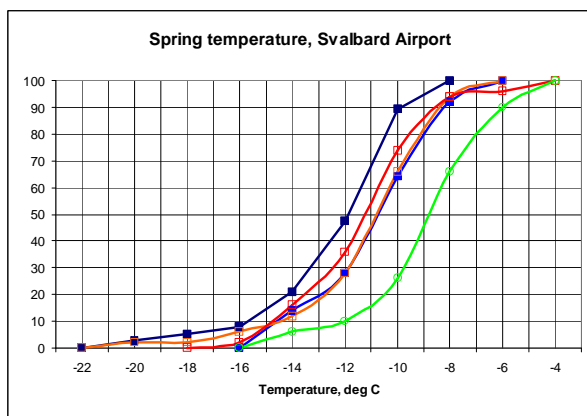
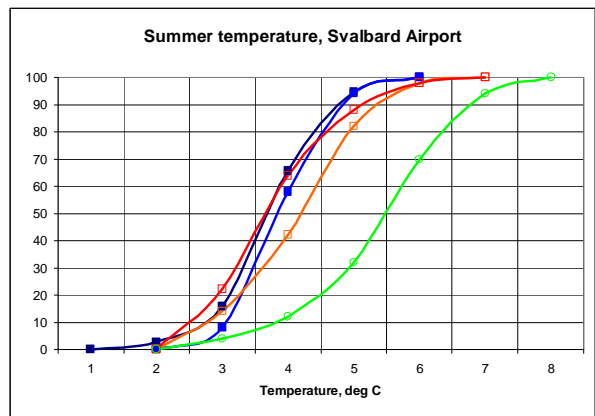
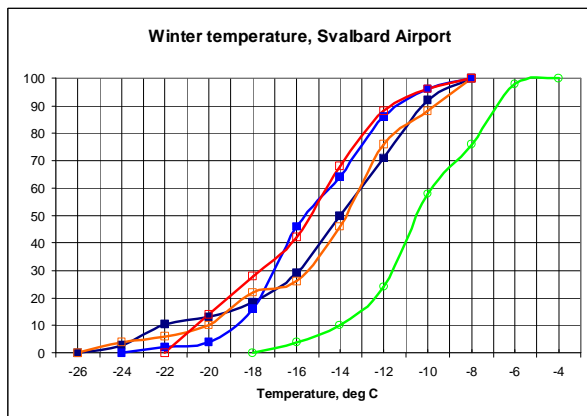
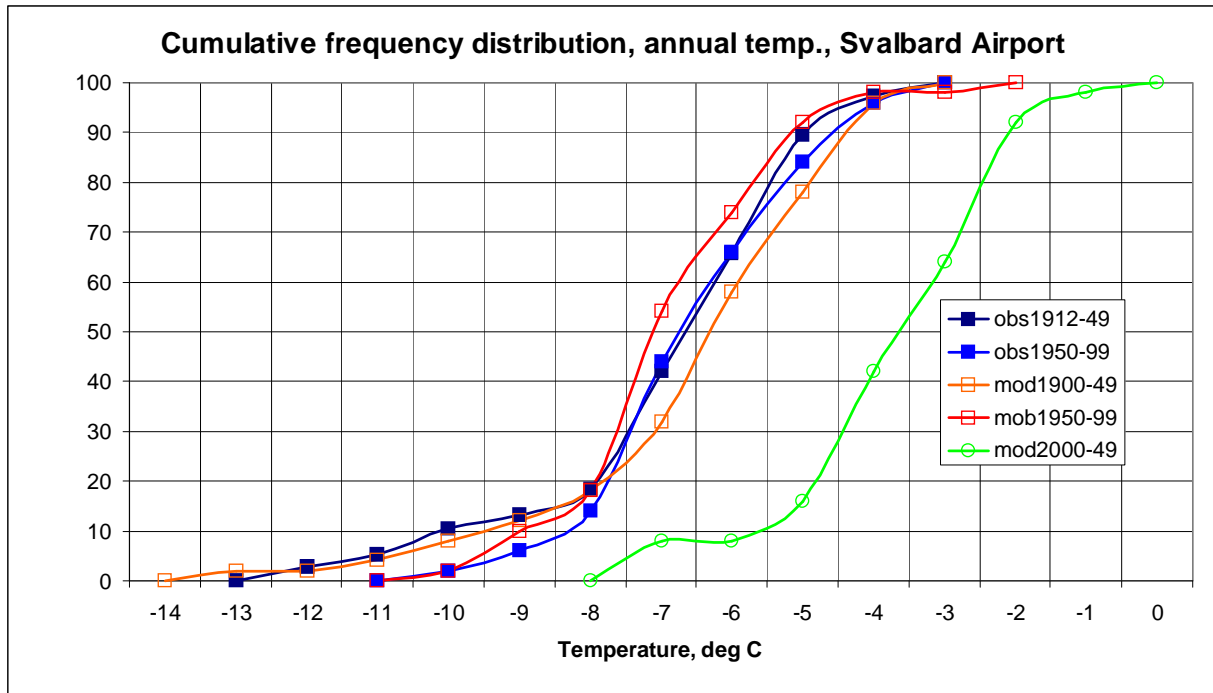


Figure 9. Cumulative frequency distributions of annual and seasonal mean temperatures at Svalbard Airport. Blue and red curves show observed and modelled distributions, respectively, based upon the periods 1900-49 (observed: 1912-49) and 1950-99. Green curves show modelled distributions for the period 2000-2049.

In Karasjok (Figure 8), observations show that the first 50-year period was considerably warmer than the second one, while the model produces two periods which both are rather similar to the second. The relatively high annual mean temperatures during the period 1900-49 were mainly due to high winter temperatures. From the present investigation it is not possible to judge whether the model potentially could produce the observed difference between two 50-year periods simply as a result from natural variability. However, the model results from Svalbard Airport (Figure 9) at least indicates that the model is able to do this. But anyway: According to the model, the next 50-year period will be considerably warmer than the warmest of the two previous ones, and the difference compared to the warmest of these two will definitely exceed the difference between them.

3.2 Time series 1900-2050 for selected stations

Filtered time series of modelled and observed annual and seasonal mean temperatures are shown in figures 10 through 16 for selected stations. Again, we emphasize that one should not compare observed and modelled curves on a year-to-year basis. Even the decadal scale variability is mainly the result of natural temperature variability, and it is thus a matter of chance whether or not this variation is in phase in model and reality. One might, however, expect that the positive long-term trends in annual mean temperatures which are found in the modelled series from the mid 1970's towards the end mainly result from the increased radiative forcing in the model, and thus should be found in the observations at least to some extent. This is also the case, especially in southern parts of Norway, but also further north.

In Northern Norway (Figures 13-15), the modelled annual trends tend to be stronger than the observed ones in the period 1975-2000, while the strongest observed positive trends during the 20th century in this area occurred before 1940. Hanssen-Bauer and Førland (1998, 2000a) showed that this trend cannot be explained by variations in atmospheric circulation alone, and they discussed (without concluding) other possible explanations. The present model results, which do not indicate any positive long-term trend during the first 50 years, support Hanssen-Bauer and Førland's rejection of increased concentration of greenhouse gases as the main reason for the warming in this period. An interesting question is if the model would be able to reproduce similar positive trends as a result from natural variability.

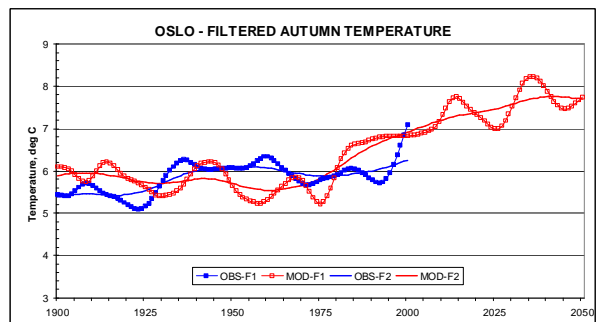
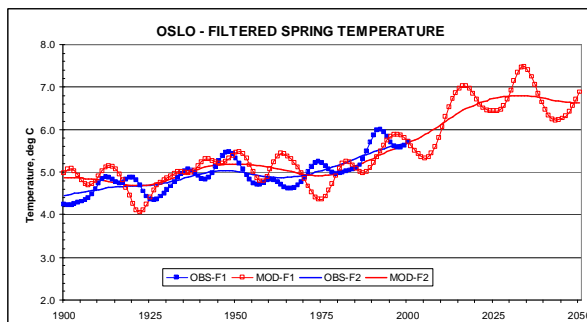
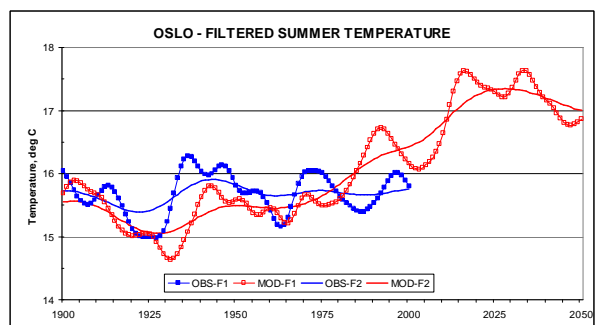
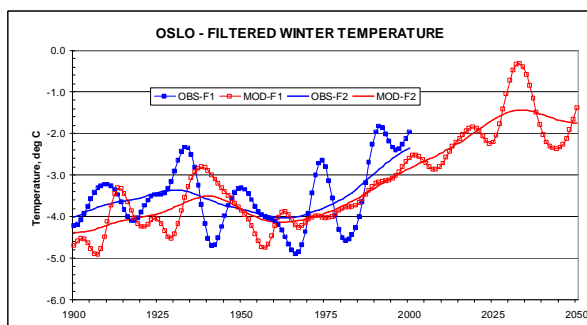
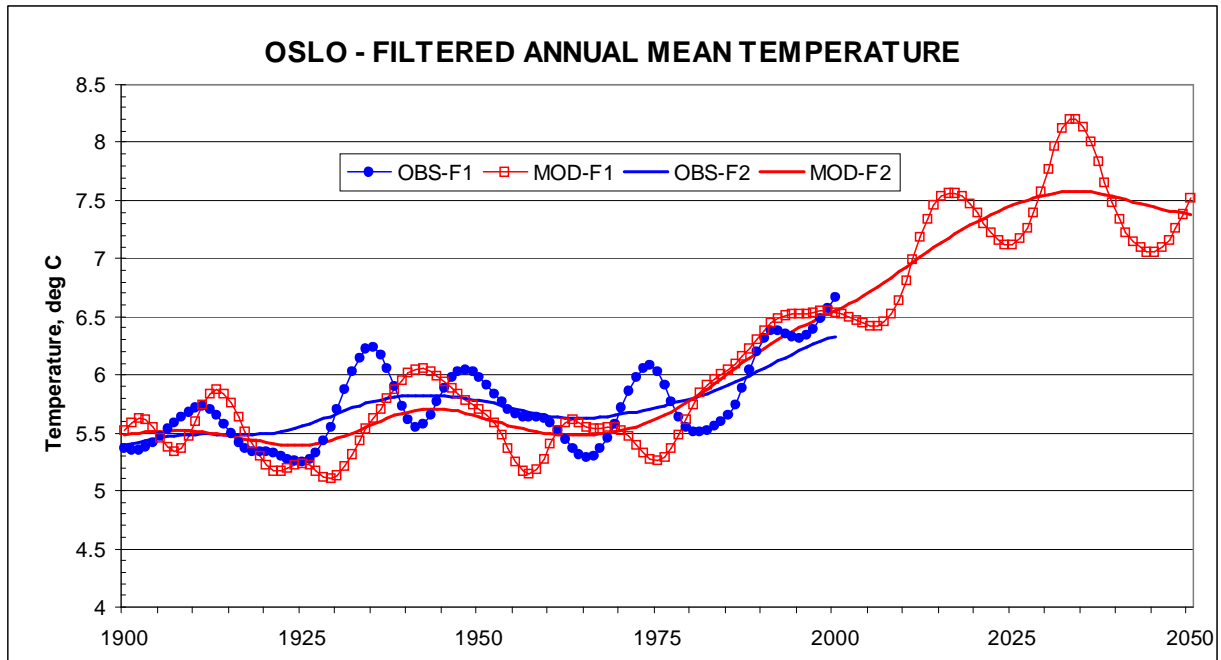


Figure10. Low-pass filtered series of annual and seasonal mean temperatures in Oslo. Observed: blue curves. Modelled: red curves. The filters, which include Gaussian distributed weights, show variation on decadal and 30-year scale approximately.

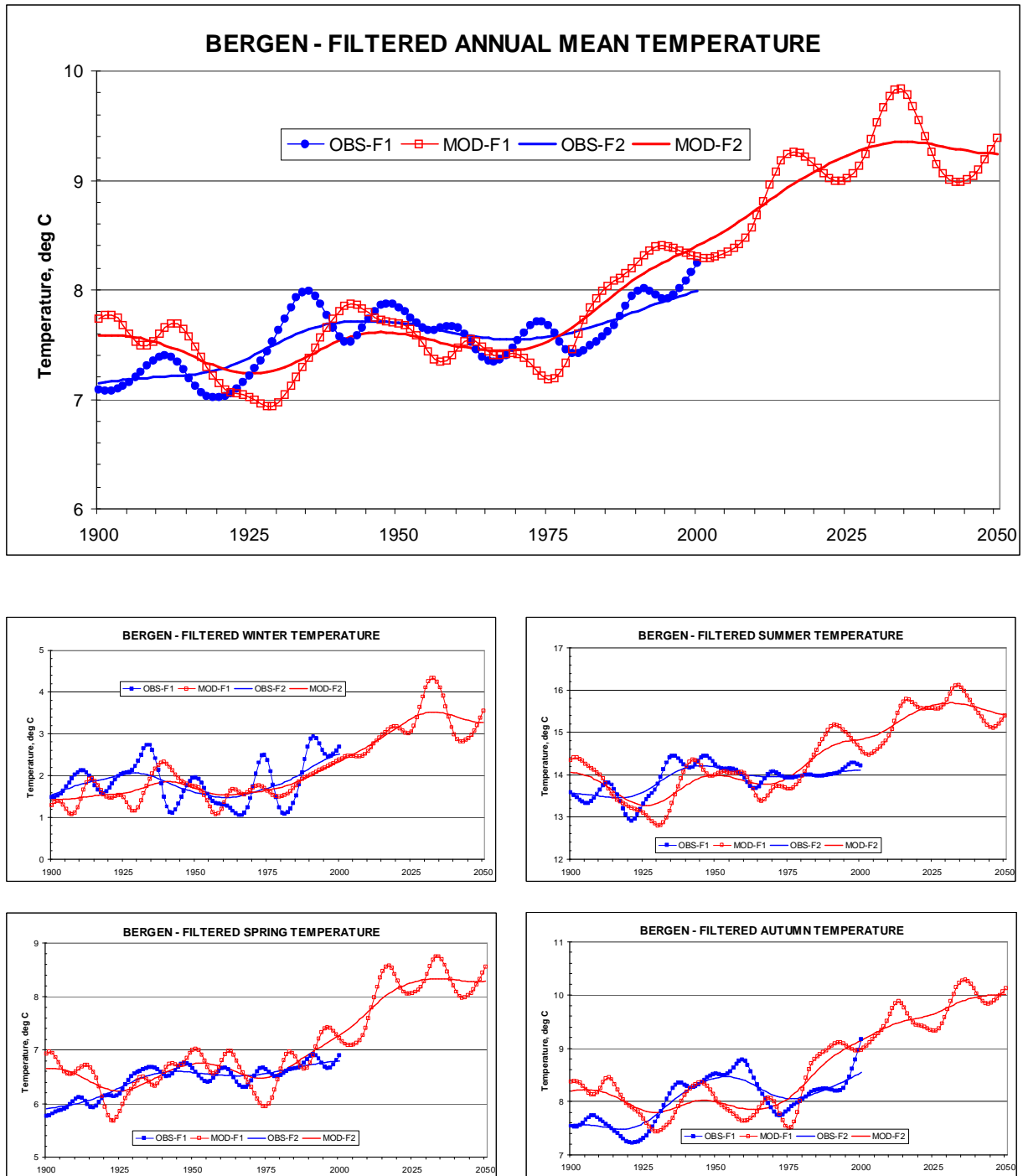


Figure 11. Low-pass filtered series of annual and seasonal mean temperatures in Bergen. Observed: blue curves. Modelled: red curves. The filters, which include Gaussian distributed weights, show variation on decadal and 30-year scale approximately.

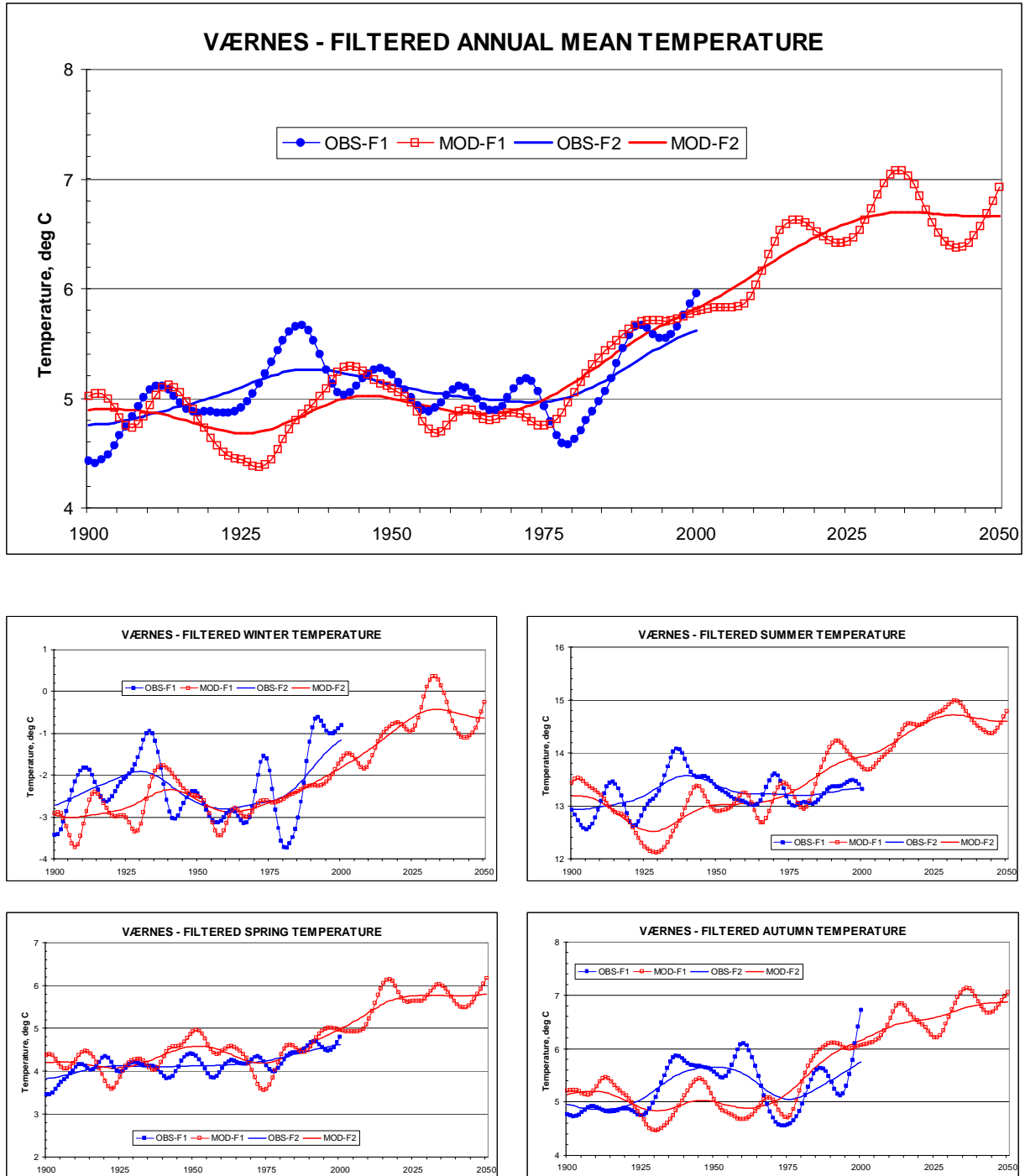


Figure 12. Low-pass filtered series of annual and seasonal mean temperatures at Værnes. Observed: blue curves. Modelled: red curves. The filters, which include Gaussian distributed weights, show variation on decadal and 30-year scale approximately.

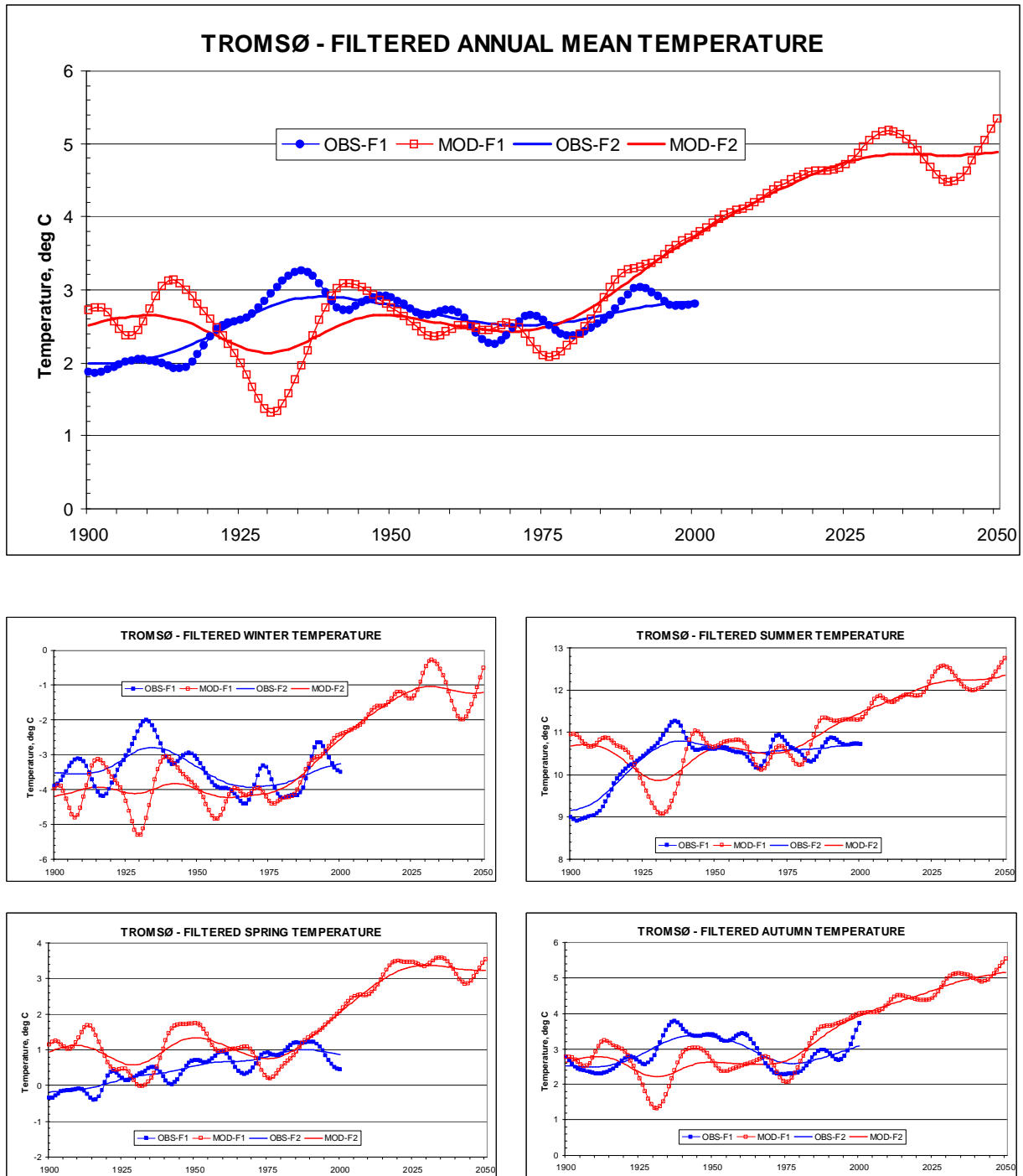


Figure 13. Low-pass filtered series of annual and seasonal mean temperatures in Tromsø. Observed: blue curves. Modelled: red curves. The filters, which include Gaussian distributed weights, show variation on decadal and 30-year scale approximately.

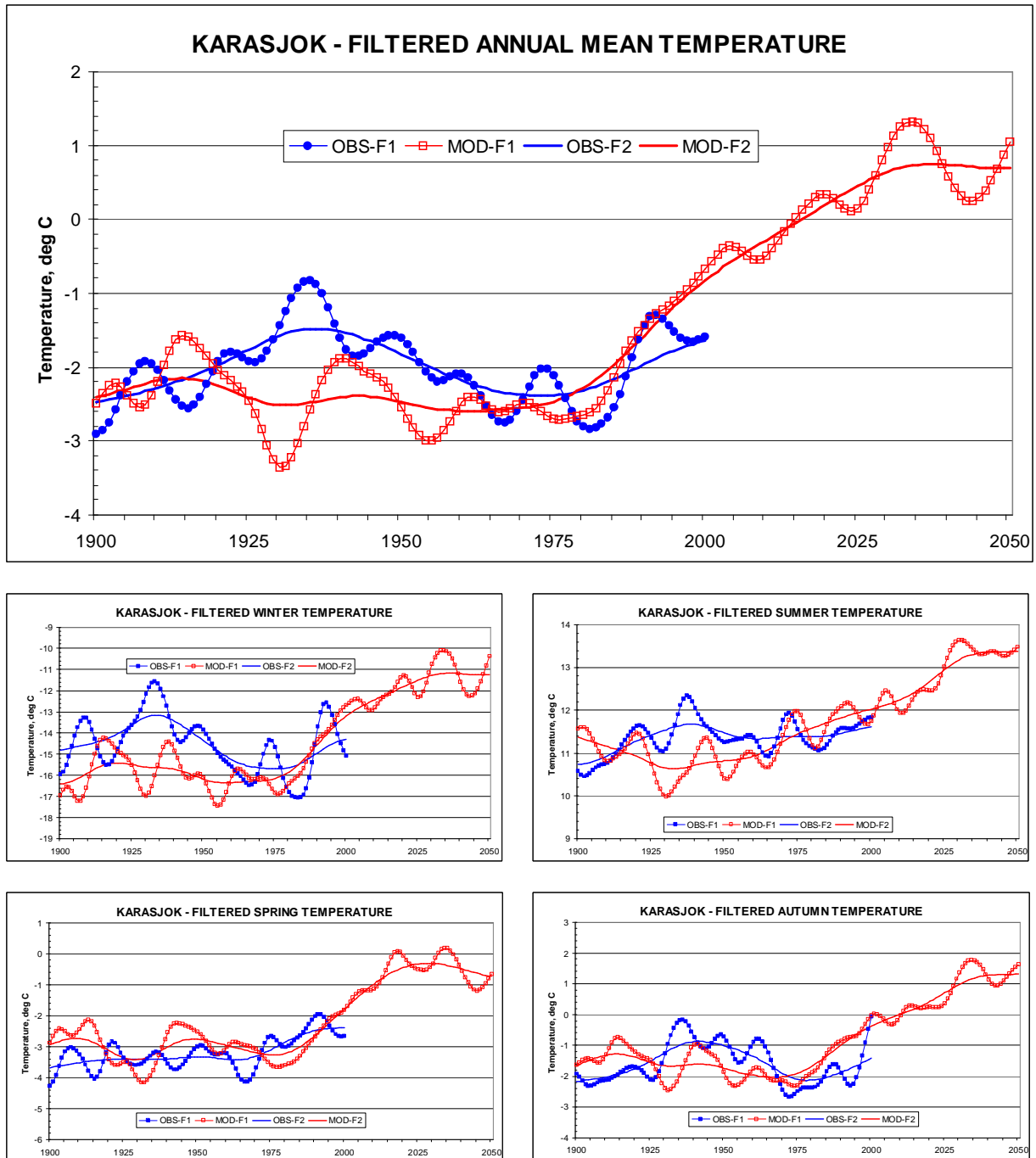


Figure14. Low-pass filtered series of annual and seasonal mean temperatures in Karasjok. Observed: blue curves. Modelled: red curves. The filters, which include Gaussian distributed weights, show variation on decadal and 30-year scale approximately.

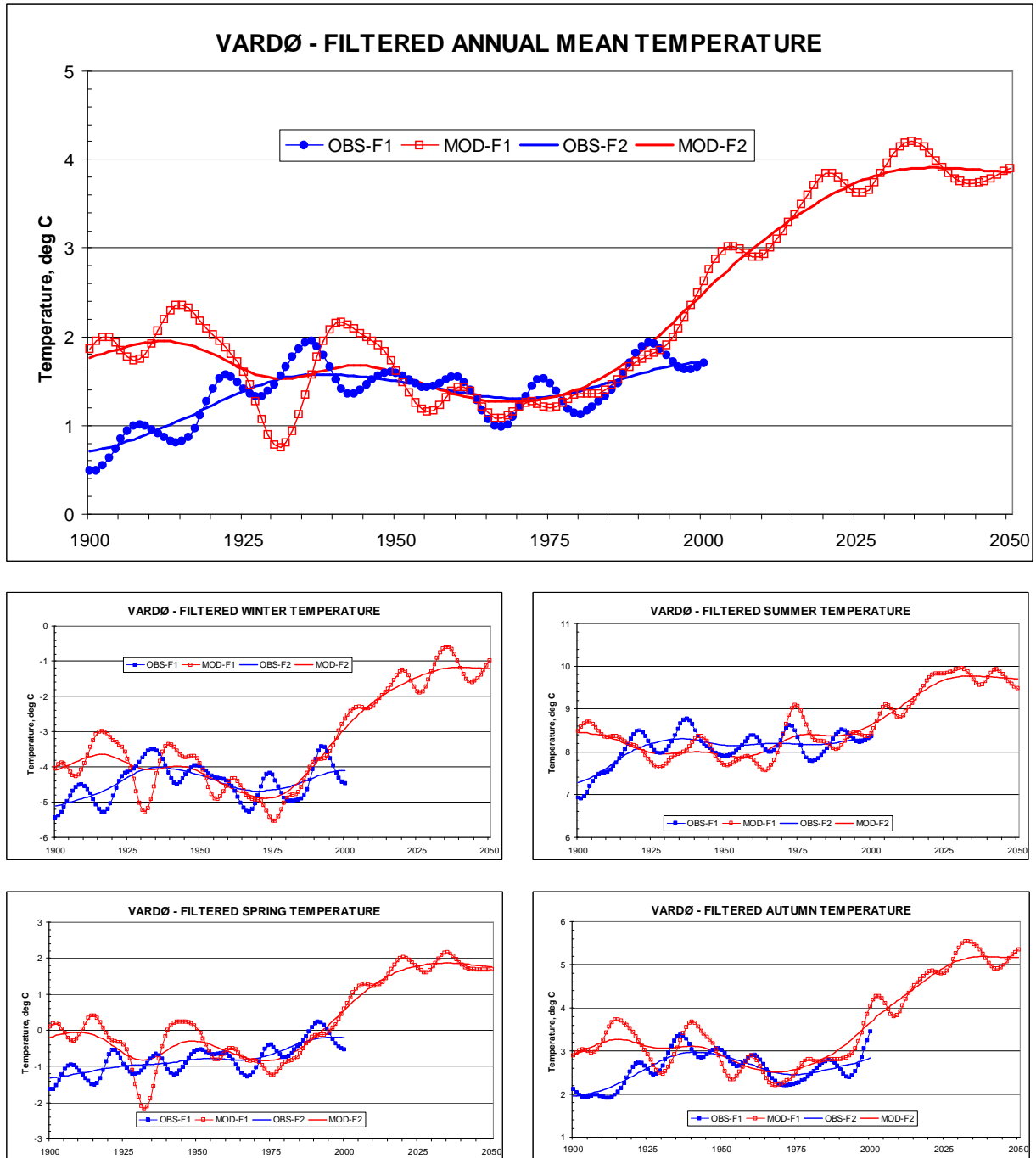


Figure 15. Low-pass filtered series of annual and seasonal mean temperatures in Vardø. Observed: blue curves. Modelled: red curves. The filters, which include Gaussian distributed weights, show variation on decadal and 30-year scale approximately.

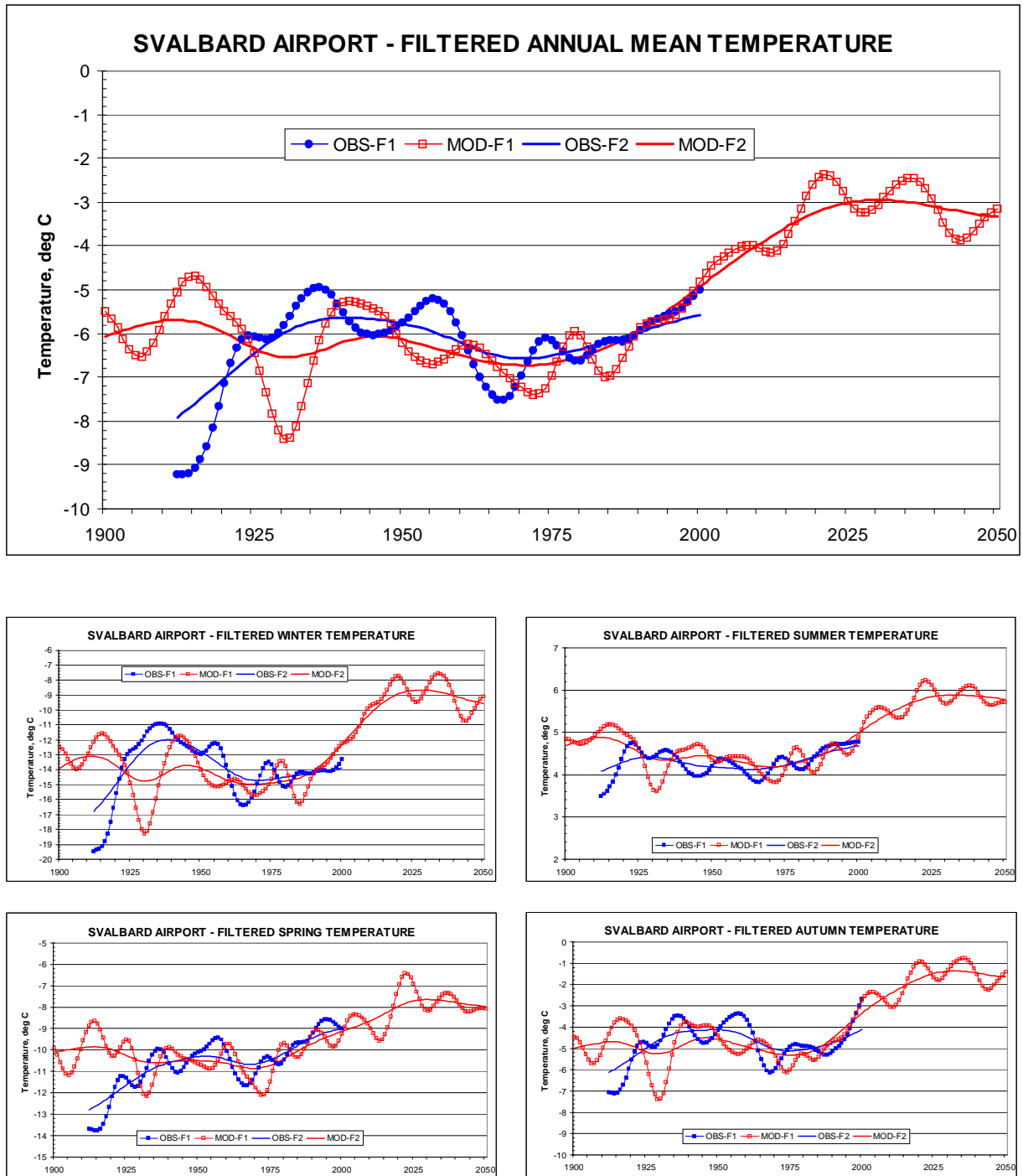


Figure 16. Low-pass filtered series of annual/seasonal mean temperature at Svalbard Airport. Observed: blue curves. Modelled: red curves. The filters, which include Gaussian distributed weights, show variation on decadal and 30-year scale approximately.

The main impression from Figures 10-16 is still that the model produces decadal scale variability with amplitudes of the magnitude we observe, and that the warming we have experienced during the latest 25 years qualitatively is in accordance with the model results.

3.3 Warming rates - definitions

Figures 10-16 make it obvious that estimates of warming rates are critically dependent on the choice of period. First, the warming rate actually changes with time (i.e. the trend it is not really linear). Secondly, the decadal scale variability is a source for uncertainty: It can make a big difference if the chosen period happens to start in a “warm” period and end in a “cold” one or vice versa . Trends should therefore always refer to a specific time interval, and they should also be given with an uncertainty interval.

There are different methods for deciding temperature increase rates: One is to calculate the linear trend during the period of interest, while another is to calculate the temperature difference between time-slices at either end of this period. The advantage of calculating the linear trend is that all data in the actual period are used. The advantage with the other method is that the time-slices then may be interpreted as two different “climatic states”, which may be used not only for calculating a temperature trend , but also for studying changes in other characteristics e.g. standard deviations or frequency distributions. In climatology, 30-years periods have traditionally been used for defining average (“normal”) climatic conditions (Førland et al., 1992). When decided internationally in 1935, the “Standard normal periods” were restricted to predefined 30-year periods, i.e. 1901-30, 1931-60, 1961-90 etc. Concerning the length of the standard normal period, one requirement was that it should be of sufficient duration to reflect climatic changes. Too long a period might prove insensitive to real climatic trends, whereas too short a period would be over-sensitive to random climatic variations. Even at that time the climatologists feared that the 11-years sunspot periods might influence climatic variations. For these reasons, they decided to operate with a period length of 30 years. The climate normals are widely used as reference values both within climatology, but also for derived values as “*growing season*”, “*heating season*”, number of “*frost days*”, number of “*summer days*”, etc.

The main temperature scenarios in the present report are thus based upon the differences between the 30-year periods 1961-90 (the latest “standard normal period”) and 2020-2049. The warming rates based upon these differences were calculated for all stations in Figure 1. They are presented in table A-3 in Appendix, with 95% confidence intervals, and they are also used for producing the maps in section 3.4. In Table 1 these warming rates (“Diff-1”) are given only for selected stations together with two other warming rate estimates. The warming rates denoted by “Diff-2” are based upon the

difference between the 20-year time-slices 1980-99 and 2030-49. The “Diff-2” rates were calculated because these 20-year time-slices were used for the dynamical downscaling over Norway (Bjørge et al. 2000), and when comparing results from dynamical and empirical downscaling (see chapter 4) it is important to use the same definition of warming rate. The third warming rate given in table 1 (“Trend”) is the linear trend from 1980 to 2049, and it was calculated because this trend was used by Benestad (2000) when comparing empirically downscaled scenarios for Norway made from different models and by various methods. Table 1 shows that the differences between the last two warming rates are small. The differences between the two last estimates and the first one, on the other hand, are occasionally considerable. The largest differences are found for summer and autumn trends at stations in southern and mid-Norway: Comparing the 30-year periods 1961-90 and 2020-49 leads to larger

*Table 1. Seasonal/annual temperature increase ($^{\circ}\text{C}$ per decade) up to 2050 calculated in 3 different ways. **Diff-1:** Increase rate based upon the difference between the 30-year periods 1961-1990 and 2020-49, with 95% confidence interval. **Diff-2:** Increase rate based upon the difference between the 20-year periods 1980-1999 and 2030-2049, with 95% confidence interval. **Trend:** Linear trend 1980-2049 with standard error.*

STATION	Method	TEMPERATURE INCREASE, $^{\circ}\text{C}$ per decade				
		WINTER	SPRING	SUMMER	AUTUMN	ANNUAL
18700 Oslo	Diff-1	0.37 ± 0.17	0.27 ± 0.14	0.26 ± 0.09	0.28 ± 0.10	0.30 ± 0.08
	Diff-2	0.36 ± 0.22	0.30 ± 0.19	0.18 ± 0.14	0.22 ± 0.09	0.26 ± 0.11
	Trend	0.36 ± 0.10	0.27 ± 0.09	0.18 ± 0.06	0.18 ± 0.06	0.24 ± 0.05
24880 Nesbyen	Diff-1	0.57 ± 0.18	0.27 ± 0.15	0.24 ± 0.10	0.32 ± 0.10	0.35 ± 0.08
	Diff-2	0.56 ± 0.34	0.29 ± 0.20	0.16 ± 0.12	0.25 ± 0.10	0.31 ± 0.14
	Trend	0.54 ± 0.16	0.27 ± 0.10	0.16 ± 0.06	0.20 ± 0.07	0.29 ± 0.06
39100 Oksøy Fyr	Diff-1	0.32 ± 0.14	0.22 ± 0.12	0.22 ± 0.08	0.24 ± 0.08	0.25 ± 0.07
	Diff-2	0.31 ± 0.19	0.25 ± 0.15	0.15 ± 0.11	0.18 ± 0.07	0.22 ± 0.09
	Trend	0.30 ± 0.09	0.23 ± 0.08	0.15 ± 0.05	0.15 ± 0.04	0.21 ± 0.04
50540 Bergen	Diff-1	0.28 ± 0.12	0.28 ± 0.11	0.28 ± 0.09	0.29 ± 0.09	0.28 ± 0.06
	Diff-2	0.29 ± 0.16	0.28 ± 0.15	0.17 ± 0.14	0.22 ± 0.08	0.24 ± 0.09
	Trend	0.28 ± 0.07	0.26 ± 0.07	0.18 ± 0.06	0.21 ± 0.05	0.23 ± 0.04
69100 Værnes	Diff-1	0.34 ± 0.14	0.24 ± 0.11	0.25 ± 0.09	0.25 ± 0.09	0.27 ± 0.07
	Diff-2	0.35 ± 0.17	0.24 ± 0.13	0.17 ± 0.14	0.18 ± 0.09	0.23 ± 0.09
	Trend	0.34 ± 0.09	0.22 ± 0.07	0.18 ± 0.06	0.15 ± 0.05	0.22 ± 0.04
82290 Bodø	Diff-1	0.43 ± 0.13	0.42 ± 0.09	0.36 ± 0.09	0.40 ± 0.11	0.41 ± 0.07
	Diff-2	0.40 ± 0.16	0.42 ± 0.12	0.30 ± 0.13	0.33 ± 0.15	0.36 ± 0.10
	Trend	0.42 ± 0.09	0.40 ± 0.07	0.30 ± 0.06	0.32 ± 0.07	0.36 ± 0.04
90450 Tromsø	Diff-1	0.48 ± 0.14	0.42 ± 0.09	0.28 ± 0.07	0.36 ± 0.10	0.39 ± 0.06
	Diff-2	0.44 ± 0.19	0.41 ± 0.12	0.23 ± 0.10	0.30 ± 0.14	0.35 ± 0.10
	Trend	0.46 ± 0.10	0.39 ± 0.07	0.24 ± 0.05	0.29 ± 0.06	0.34 ± 0.04
97250 Karasjøk	Diff-1	0.79 ± 0.23	0.44 ± 0.12	0.33 ± 0.13	0.48 ± 0.13	0.51 ± 0.08
	Diff-2	0.67 ± 0.34	0.47 ± 0.18	0.34 ± 0.19	0.45 ± 0.18	0.48 ± 0.14
	Trend	0.67 ± 0.17	0.43 ± 0.10	0.33 ± 0.09	0.45 ± 0.08	0.47 ± 0.07
98550 Vardø	Diff-1	0.58 ± 0.11	0.42 ± 0.06	0.27 ± 0.10	0.43 ± 0.07	0.42 ± 0.05
	Diff-2	0.57 ± 0.15	0.44 ± 0.08	0.30 ± 0.13	0.46 ± 0.11	0.44 ± 0.07
	Trend	0.55 ± 0.07	0.41 ± 0.05	0.29 ± 0.07	0.44 ± 0.05	0.42 ± 0.04
99840 Svalbard Airport	Diff-1	0.99 ± 0.27	0.52 ± 0.20	0.29 ± 0.09	0.62 ± 0.16	0.61 ± 0.14
	Diff-2	1.18 ± 0.38	0.46 ± 0.25	0.33 ± 0.14	0.71 ± 0.25	0.67 ± 0.19
	Trend	1.11 ± 0.18	0.41 ± 0.14	0.29 ± 0.07	0.66 ± 0.12	0.62 ± 0.10

trends than the two estimates made for the period 1980-2049. The trend estimates thus seem to be more sensitive to the choice of period than to the choice of method. From Figures 10-12, it is obvious that the differences between the trends are caused by the strong warming found around 1980 in the curves describing decade scale variability.

3.4 Warming rates from 1961-1990 to 2020-2049

Figures 17 through 21 show the modelled warming rates in Norway based on the difference between the two 30 year periods on annual and seasonal base, respectively. The lowest annual warming rates (about 0.2 °C per decade) are found along the coast of southern Norway, while the rates generally increase when moving inland and to the north. The largest warming rates on an annual basis are found at the Arctic stations (about 0.6 °C per decade). On the mainland the largest rates are found in the northern inland (about 0.5 °C per decade).

Concerning seasonal warming rates, there are also large differences: Along the coast of South- and Mid-Norway (especially the west-coast), there are generally small differences in the expected seasonal warming rates. In the inland and further north, however, the strongest warming is definitely expected during the winter. The map of winter warming rates (Figure 18) thus shows strong gradients from the west-coast values of 0.2-0.3 °C per decade to the inland and the north, where rates of more than 0.7 °C per decade can be found. In summer (Figure 20) on the other hand, no warming rate, even in the Arctic, exceeds 0.4 °C per decade, and the map show only weak spatial gradients.

In winter, one should note that strong gradients are found, not only from coast to inland, but also between different inland stations. At the mountain station “Gaustatoppen”(1828 m a.s.l.), the winter warming rate is about 0.3 °C per decade, while it is almost twice as high at the valley station “Nesbyen”, less than 100 km away. The reason why empirical downscaling gives this result is obviously that “warm winters” historically have been, relatively speaking, “warmer” at the valley station than on the mountain. The physical reason for this, is that temperature inversions (which are common in the valleys during winter) generally have been weaker and/or less frequent in mild winters than in other winters, at least partly because mild winters in Norway so far have been associated with increased cyclone activity, where wind and clouds have restrained the formation of inversions. Cold winters, on the other hand, have been associated with blocking situations with calm and clear weather which is favourable for the formation of inversions. An interesting question is if the predicted future warming also will be associated with increased cyclone activity over Norway in winter. In that case, the above results are probably realistic, but in the opposite case, empirical downscaling may give misleading results. This question will be discussed further in chapter 4.

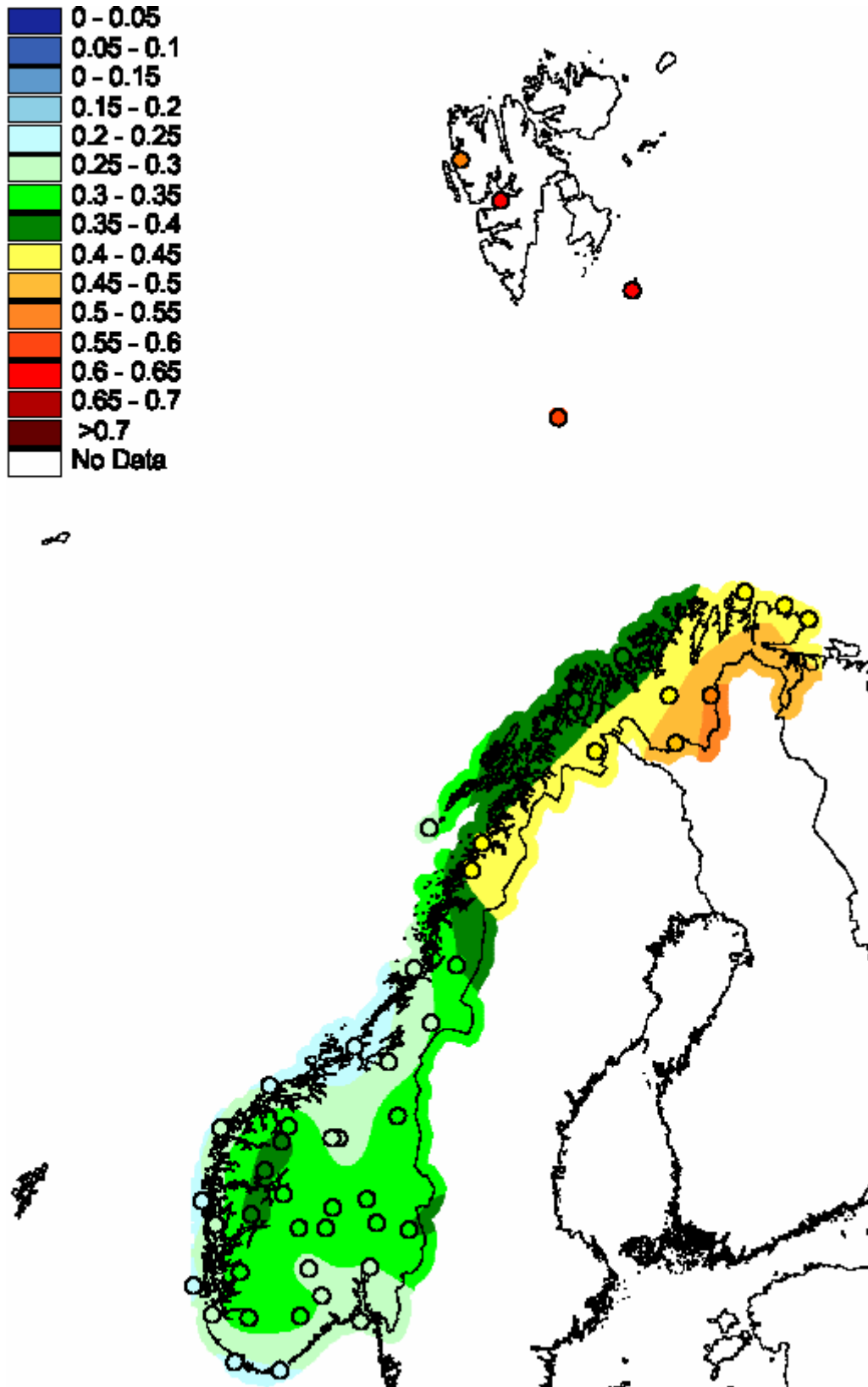


Figure 17. Results from empirical downscaling: Increase in annual mean temperature per decade from the period 1961-1990 to the period 2021-2050.

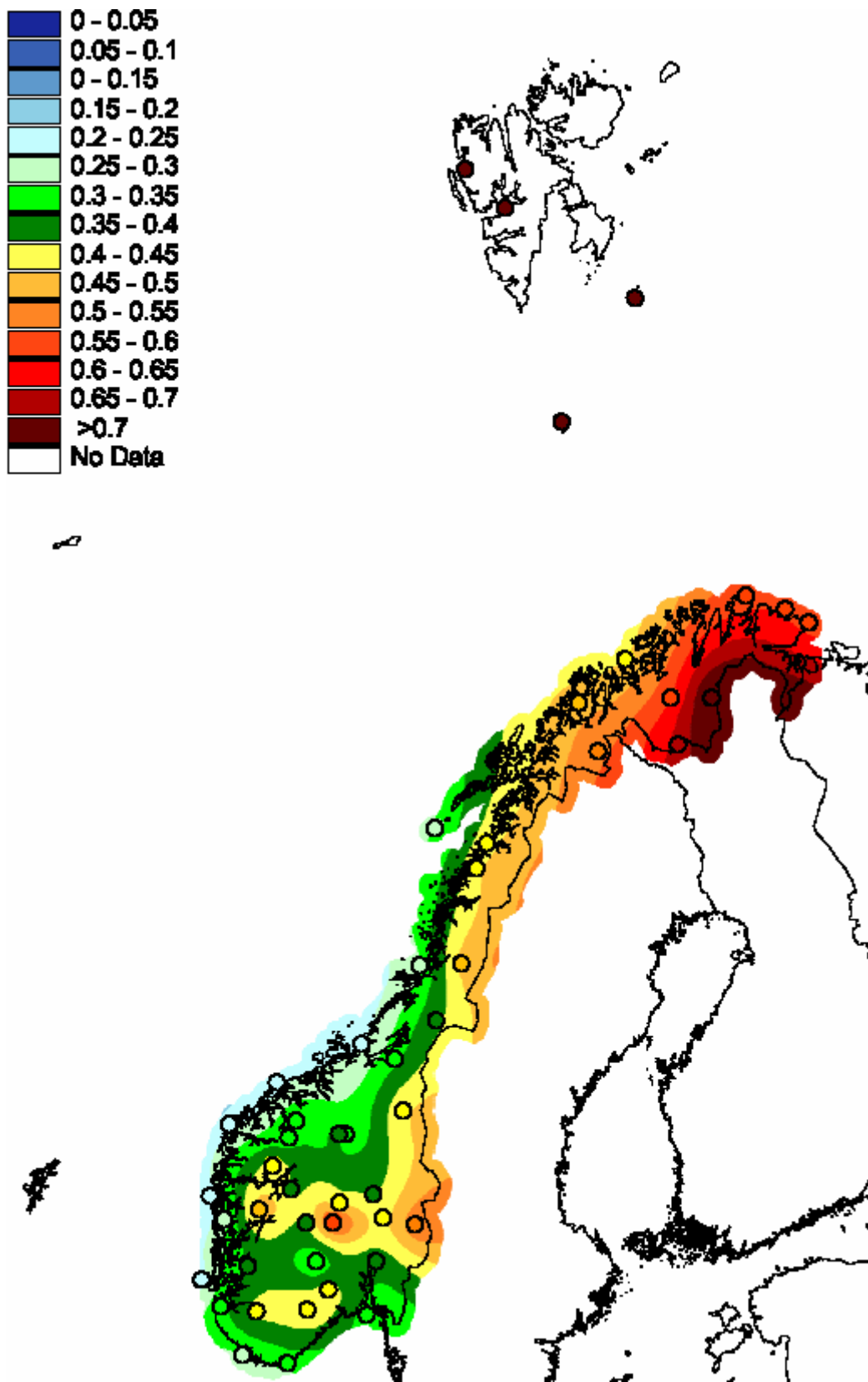


Figure 18. Results from empirical downscaling: Increase in winter temperature (Dec-Jan-Feb) per decade from the period 1961-1990 to the period 2021-2050.

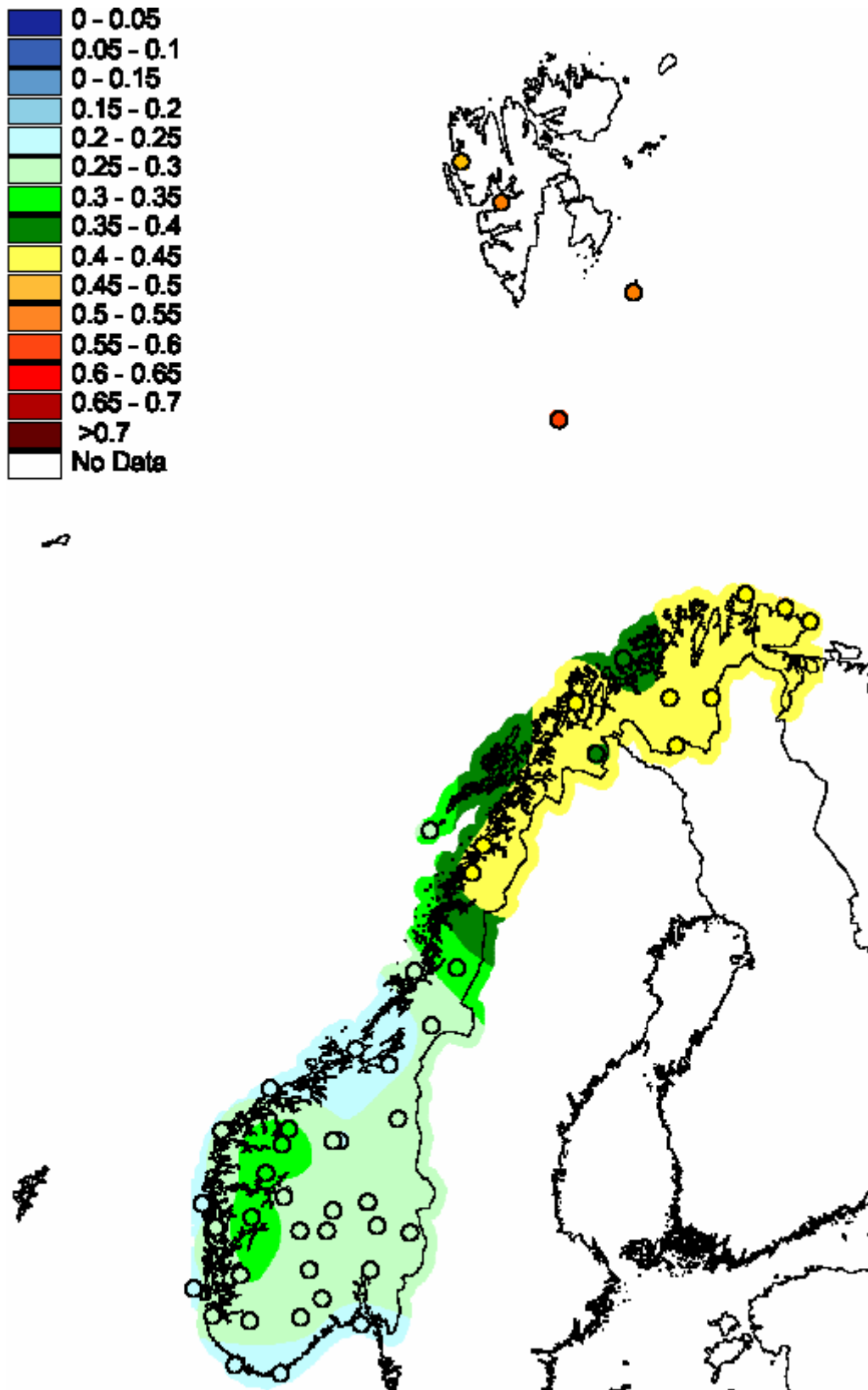


Figure 19. Results from empirical downscaling: Increase in spring temperature (Mar-Apr-May) per decade from the period 1961-1990 to the period 2021-2050.

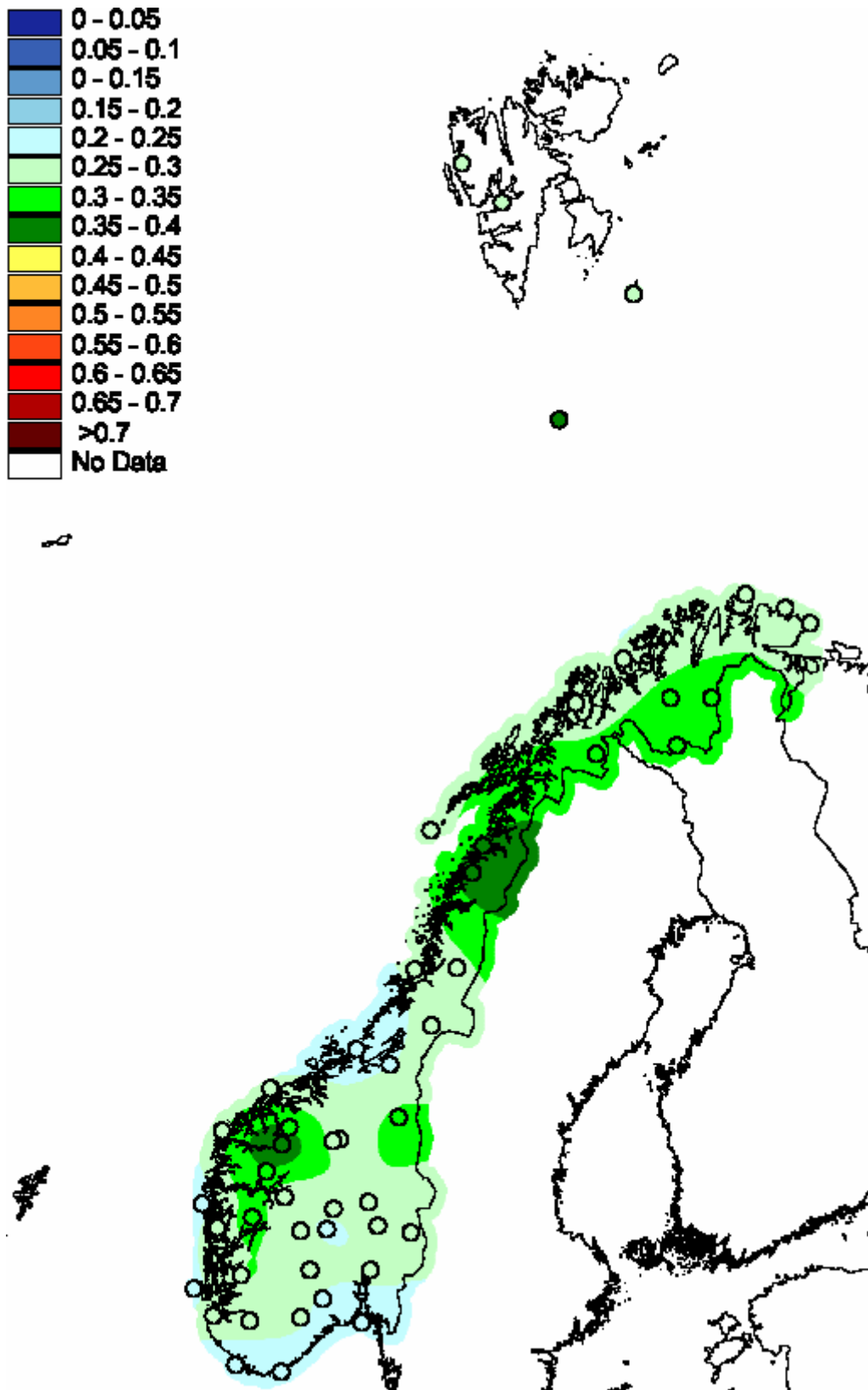


Figure 20. Results from empirical downscaling: Increase in summer temperature per decade from the period 1961-1990 to the period 2021-2050.

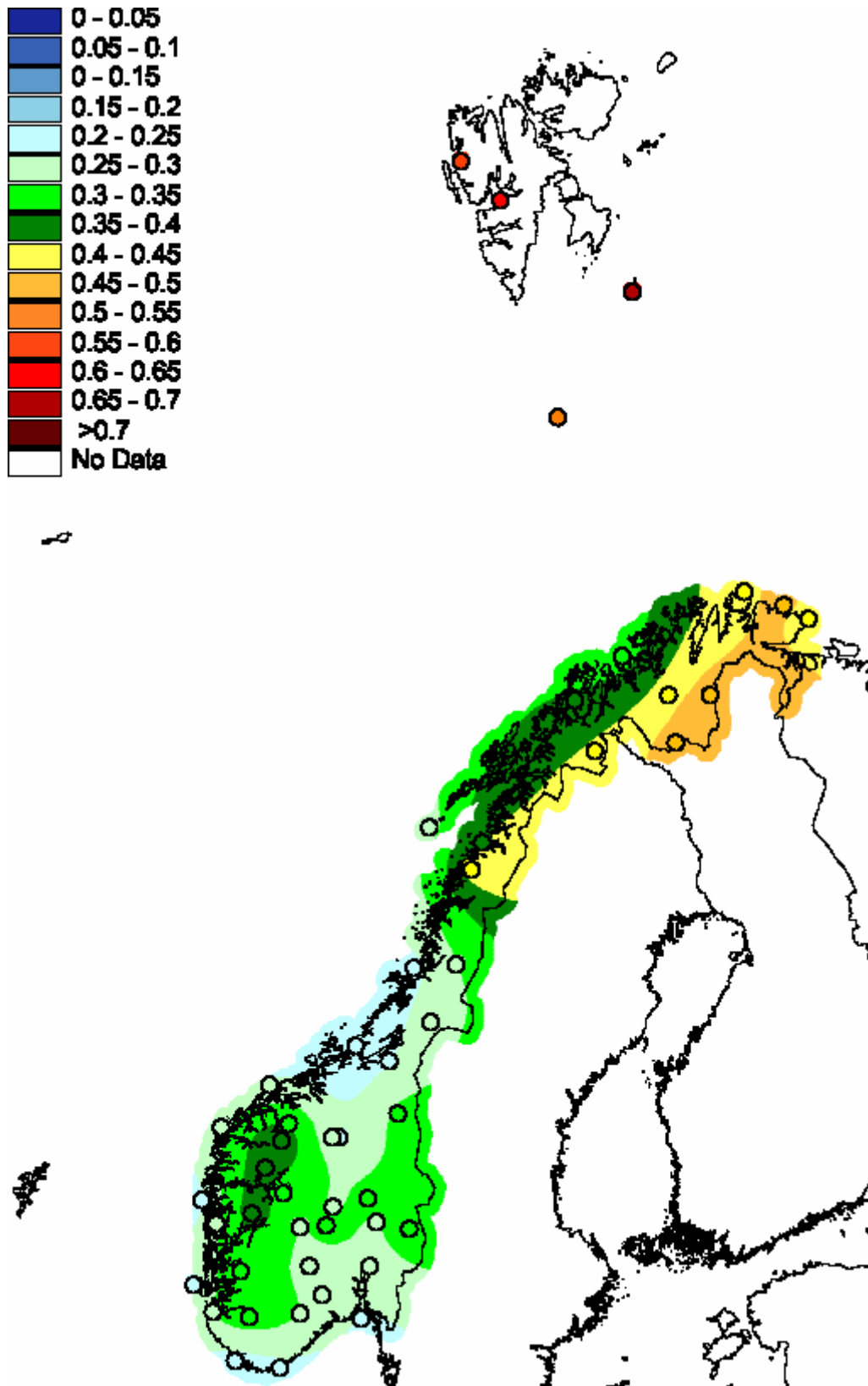


Figure 21. Results from empirical downscaling: Increase in autumn temperature per decade from the period 1961-1990 to the period 2021-2050.

In addition to comparing temperature means for the periods 1961-1990 and 2020-49, we looked for systematic changes in the temperature standard deviations. The last rows in Tables A-2 a) through l) (Appendix-2) show standard deviations of the monthly mean temperatures for the period 2020-2049. When comparing these values to the similar values for the previous 30-year periods, it is obvious that the natural variability in the standard deviations in most cases is too large to mask eventual systematic changes. There seem to be a tendency for reduced standard deviations in November and February at inland stations like Nesbyen and Karasjok. The only clearly significant change, however, is found at the Arctic stations: The standard deviations for the winter months decrease at all these stations, while they at Bjørnøya decrease also in spring and autumn. The reason for this is probably that the reduction in the sea-ice extent which gives fewer of the extremely cold winters.

3.5 Scenarios for changes in derivative characteristics

Because the 30-year climatic averages form an international standard, several empirical relations have been developed between them and other characteristics, which thus may be derived if these “normal values” are known. Examples of such derivative characteristics are “heating season” and “growing season”. A separate report will be published, where the present temperature scenarios will be used for calculating changes in these characteristics all over the country. In the present section, only a few examples are given.

Table 2 shows changes in length of heating season at a few stations. The heating season is defined as the period from the date when the mean daily temperature falls below 11 °C during the autumn and till the date when it rises to above 9 °C during the spring. The “standard heating season” is based on a smoothed curve for mean daily temperatures for a standard normal period of 30 years. Table 2 shows that the largest decreases in length of heating season are found at Finnmarksvidda (Karasjok), and in coastal areas in Western Norway (Bergen).

Table 2. Changes in length of “standard heating season” from (1961-90) to (2020-49)

		Start		End		Δ Length (days)
		(1961-90)	(2021-50)	(1961-90)	(2021-50)	
11500	Østre Toten	03.sep	10.sep	16.may	10.may	-13
18700	Oslo-Blindern	14.sep	23.sep	07.may	30.apr	-16
24880	Nesbyen	01.sep	07.sep	16.may	09.may	-13
50540	Bergen-Florida	17.sep	11.okt	06.may	25.apr	-35
69100	Værnes	04.sep	12.sep	15.may	07.may	-16
97250	Karasjok	15.aug	22.aug	09.jun	22.may	-25

The growing season is in this context defined as the period when the smoothed daily mean temperature for a 30-year period is above 5 °C. Table 3 indicates that in the Oslo area and at Finnmarksvidda, the growing season will last 3 more weeks during 2021-50 than presently. In the Bergen-region the lawns have to be cut during more than a month longer period than compared to present day conditions!

Table 3. Changes in length of "standard growing seasons" from (1961-90) to (2020-49)

		Start		End		Δ Length (days)
		(1961-90)	(2021-50)	(1961-90)	(2021-50)	
11500	Østre Toten	29.apr	21.apr	15.oct	25.oct	18
18700	Oslo-Blindern	19.apr	09.apr	24.oct	04.nov	21
24880	Nesbyen	27.apr	18.apr	10.oct	20.oct	19
50540	Bergen-Florida	07.apr	18.mar	12.nov	26.nov	34
69100	Værnes	24.apr	16.apr	21.oct	30.oct	17
97250	Karasjok	22.may	08.may	17.sep	26.sep	23

4. Comparisons between empirical and dynamical downscaling

Results from dynamical downscaling from the same ECHAM4/OPYC3 integration that was used as input in the present empirical downscaling, were presented by Bjørge et al. (2000). Typical regional warming rates based upon their downscaling of the two time-slices 1980-1999 and 2030-2049 are shown in table 4. When compared to the maps in the previous section, the warming rates in table 4 seem, at the best, to give the lower limit of the values found at the maps. In summer and autumn, however, most of the differences are caused by the differences concerning time-slices (cf. the different warming rates in table 1). As we here want to isolate the differences in downscaling results which are connected to the choice of technique (empirical vs. dynamical), it is thus important to compare warming rates based upon the temperature difference between the same time-slices. The maps shown in Figures 22 – 26 thus show the differences in warming rates between the present empirical downscaling and the Bjørge et al. (2000) dynamical downscaling, when both are referring to the time-slices 1980-1999 and 2030-2049.

Table 4. Seasonal/annual temperature increase (°C per decade) from 1980-99 to 2030-49, Results from dynamical downscaling (Bjørge et al., 2000)

	WINTER	SPRING	SUMMER	AUTUMN	ANNUAL
South-East Norway	0.26	0.20	0.12	0.26	0.22
South-West Norway	0.24	0.18	0.14	0.22	0.20
Northern Norway	0.40	0.28	0.24	0.34	0.32

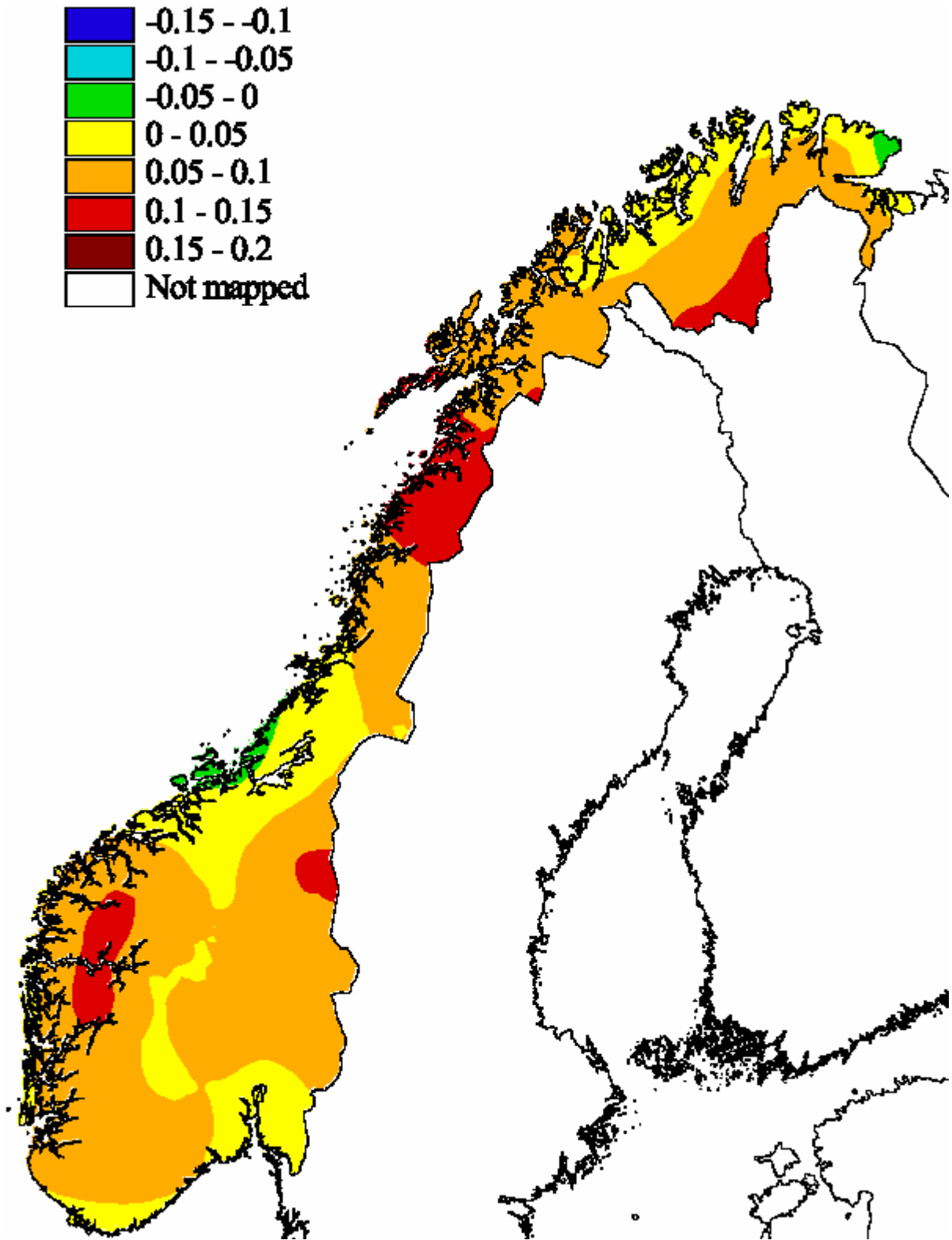


Figure 22. Differences (E-D) in the (1980-99) to (2030-2049) annual warming rates based upon empirical (E) and dynamical (D) downscaling. Unit: °C per decade

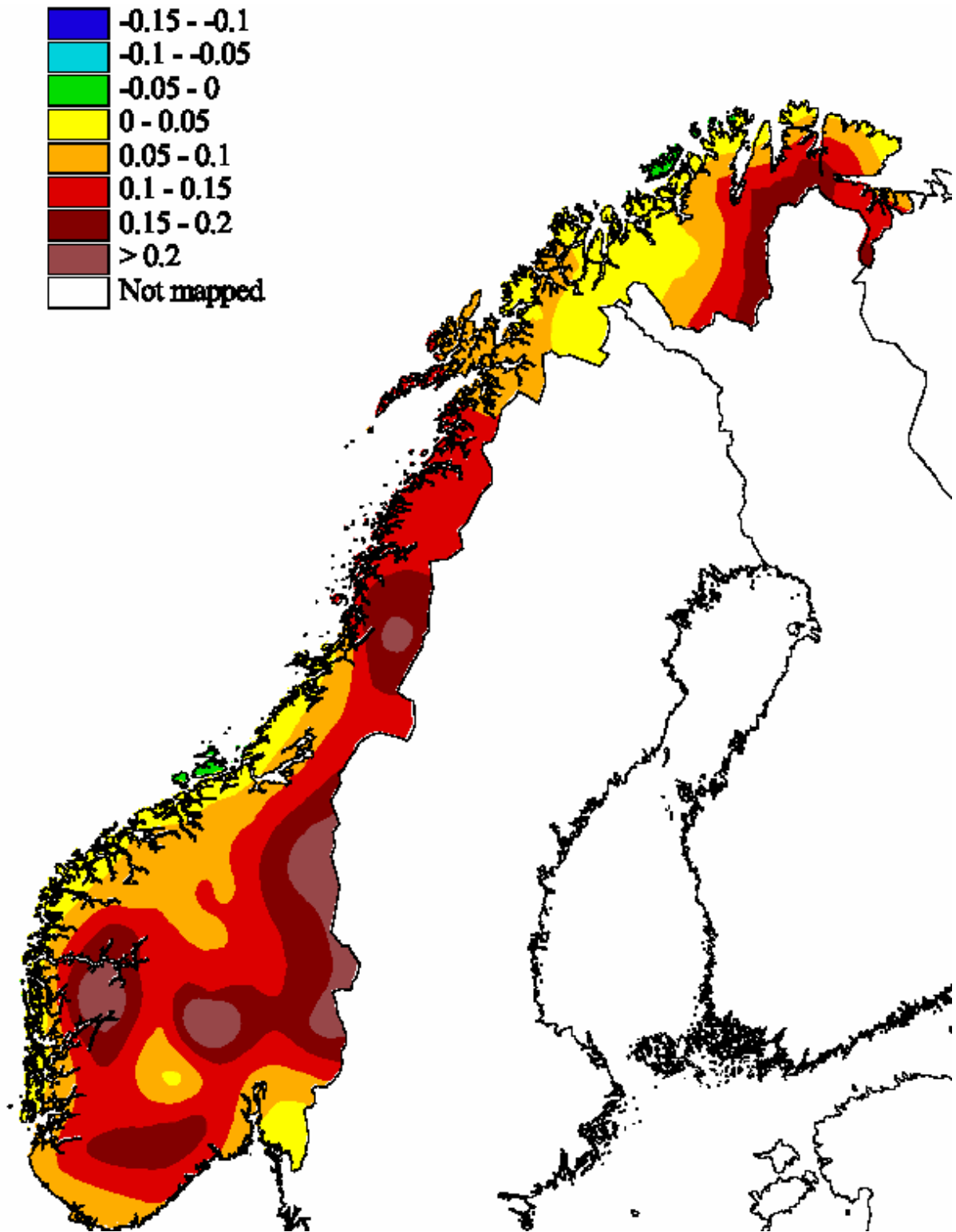


Figure 23. Differences (E-D) in the (1980-99) to (2030-2049) winter warming rates based upon empirical (E) and dynamical (D) downscaling. Unit: °C per decade

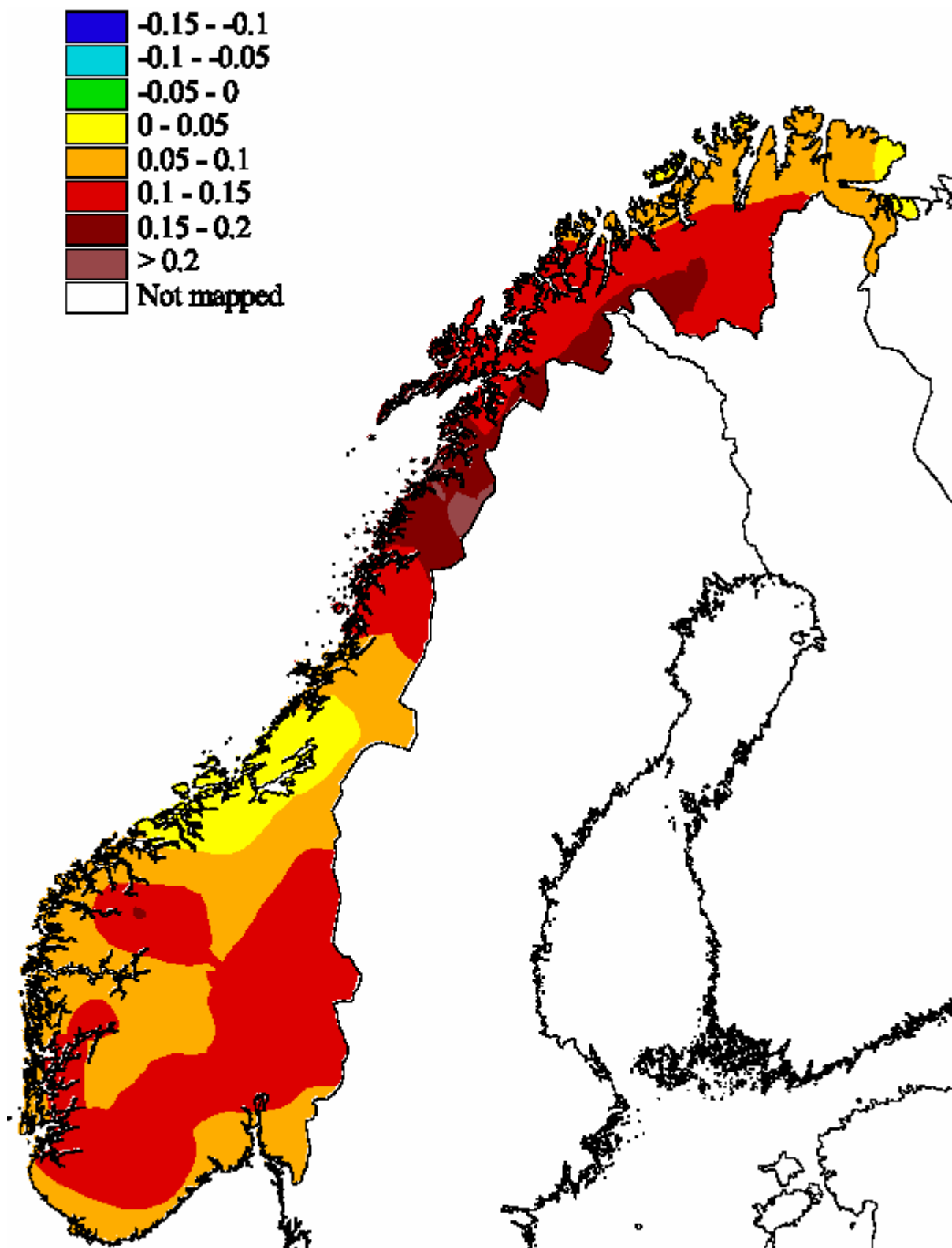


Figure 24. Differences (E-D) in the (1980-99) to (2030-2049) spring warming rates based upon empirical (E) and dynamical (D) downscaling. Unit: °C per decade

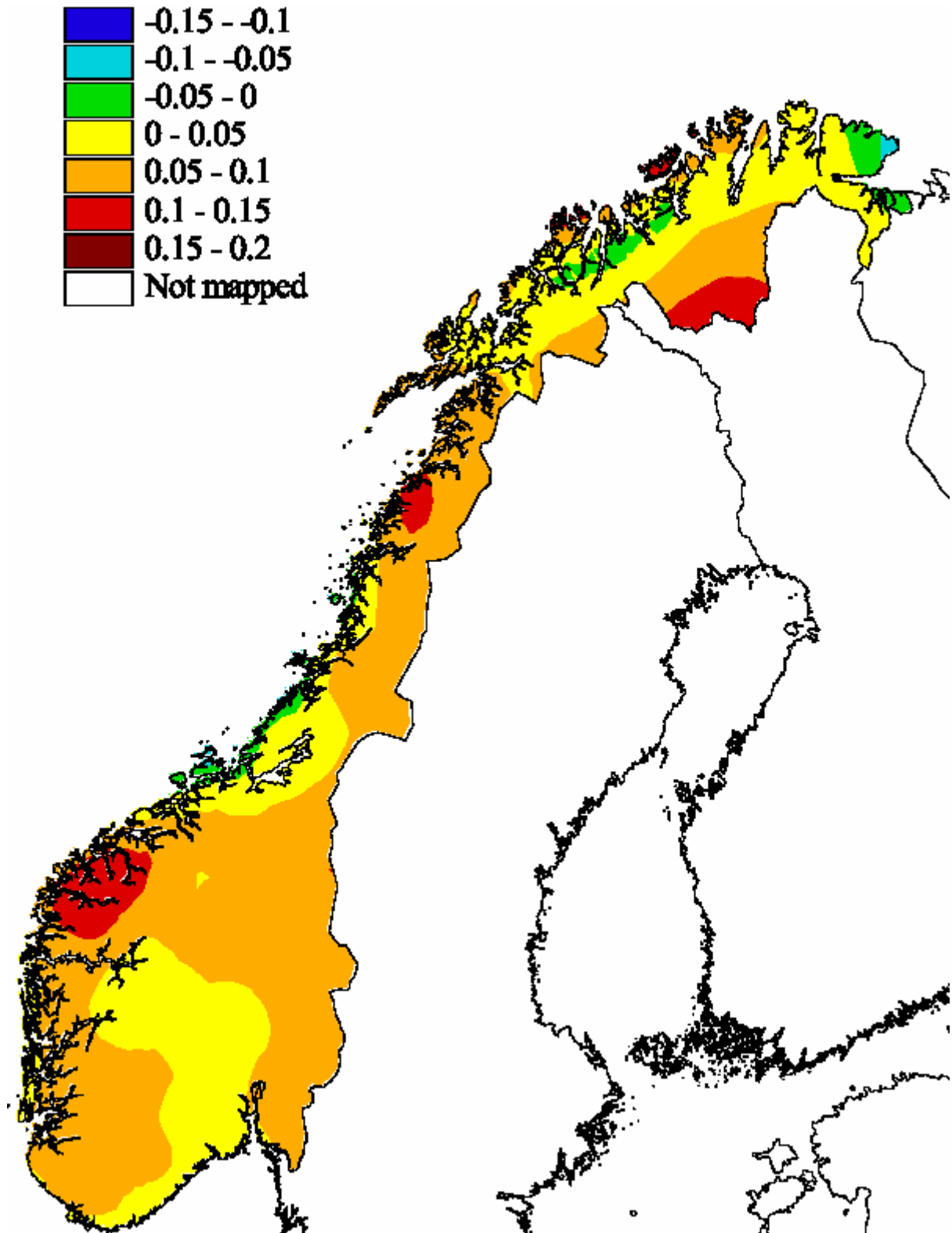


Figure 25. Differences (E-D) in the (1980-99) to (2030-2049) summer warming rates based upon empirical (E) and dynamical (D) downscaling. Unit: °C per decade

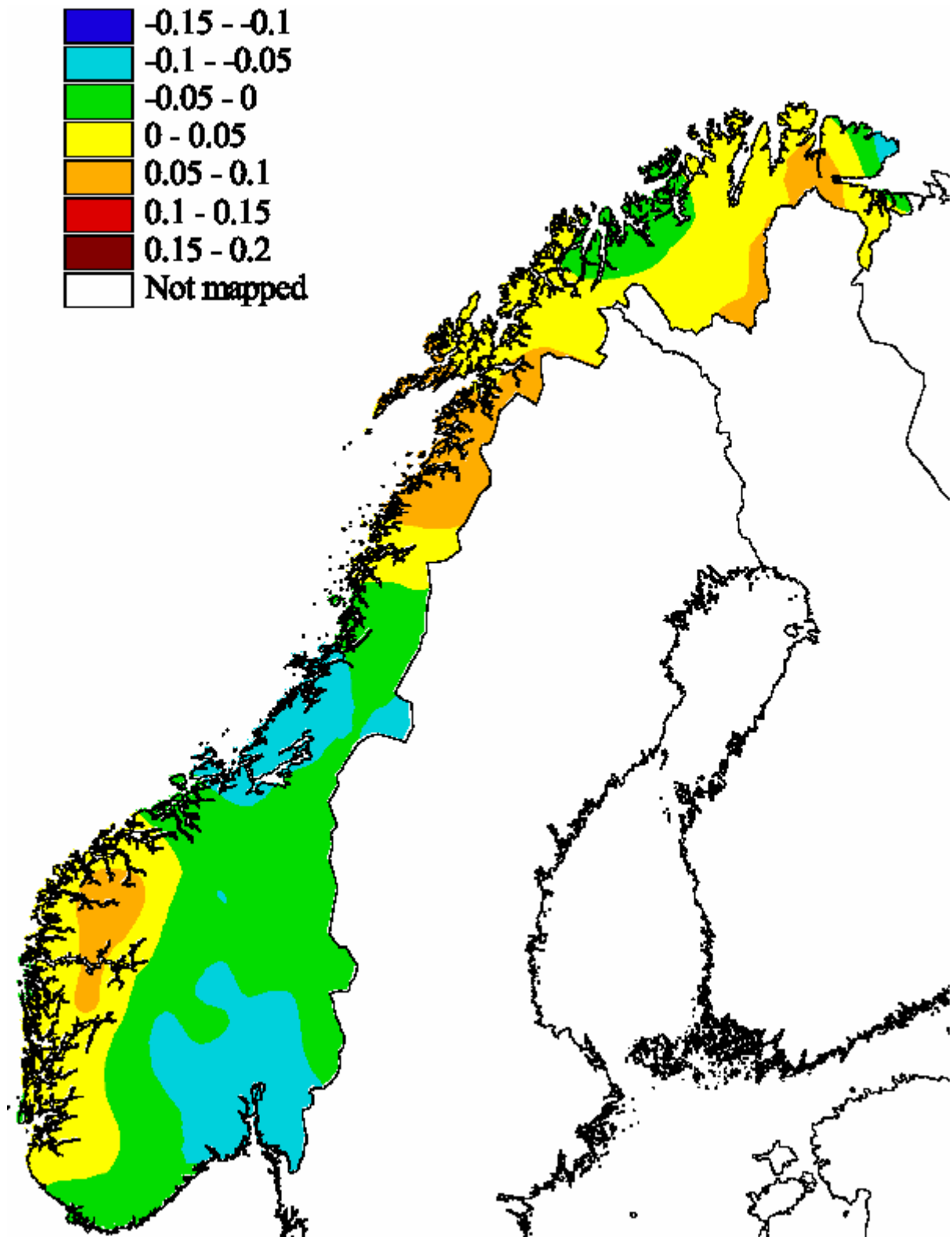


Figure 26. Differences (E-D) in the (1980-99) to (2030-2049) autumn warming rates based upon empirical (E) and dynamical (D) downscaling. Unit: °C per decade

In summer and autumn (Figures 25-26) the differences between the two estimates are, with very few exceptions, less than $\pm 0.1^{\circ}\text{C}$ per decade. In autumn, the dynamical downscaling gives slightly higher warming in the south-east, while the empirical downscaling gives slightly higher warming in the south-west and in most parts of northern Norway. In summer, empirical downscaling gives slightly stronger warming in most parts of the country.

In winter and spring (Figures 23-24), however, the differences between the two estimates are generally larger. With very few exceptions, empirical downscaling gives larger warming than dynamical downscaling, and the differences typically increase from small values along the coast to larger values in the inland. The differences are particularly large at valley stations, where they in winter may exceed 0.2°C per decade.

Note that difference between the warming rates at the mountain top station “Gaustatoppen” in winter is still below 0.05°C per decade! This indicates that the main difference between the warming rates from the empirical and the dynamical downscaling are connected to inversion-exposed inland areas. A question is thus which method that is supposed to be most reliable in these areas. The topographical resolution applied in the dynamical downscaling is too coarse to dissolve ground inversions. Thus: If some of the winter warming in the inland really is connected to the reduction of ground inversion, the dynamical downscaling model would not be able to include this part of the warming. On the other hand: The empirical downscaling technique implies the assumption that the future winter warming will follow the patterns which are found in warm winters in the past, i.e. that the warming will not be “uniform”, but that ground inversions in valleys and on plains will be weakened, and the warming thus will be larger in valleys than on mountain tops. So the question is if this is a reasonable assumption.

Hanssen-Bauer and Førland (2000b) showed that the GSDIO integration at average gives a strengthened north-south pressure gradient over Norway during the scenario period. Bjørge et al. (2000) concluded that the results from the dynamical downscaling give an increase, both in average mean 10 m wind-speed and in precipitation, and that these probably are connected to larger cyclonic activity in the area. Knippertz et al. (2000) concluded that also the GHG integration with the ECHAM4/OPYC3 gives increase in wind speeds and cyclonic activity in winter. It thus seems reasonable that the future winter warming will be accompanied by increased average wind speeds and cloud cover, which most likely will lead to weaker and/or less frequent inversions. Also the expected general reduction of the period with snow covered ground will make the conditions less favourable for ground inversions. We thus conclude that the results from the empirical downscaling, which include higher winter warming rates in valleys and at other inversion exposed locations than in the mountains and along the coast, probably are qualitatively right. Of course it is still possible that the empirical

downscaling technique exaggerates this effect, but the method has probably captured a real effect, which presently cannot be resolved by the dynamical method.

There is an area in Nordland and Troms county where the differences in winter- and spring- warming rates are large, even along the coast. The station coverage is rather poor in this area, and the stations may be unrepresentative for the area. The results from the dynamical downscaling may thus be more reliable than the present results here. Generally, the success of empirical downscaling techniques dependent critically on the availability of long, high quality series of observations. In areas with few such series, dynamical downscaling techniques probably give better results.

The differences between the two estimates may seem large, as they frequently exceed a third of the warming rate itself. Note that the differences still in most cases are within the 95% confidence intervals given for “Diff-2” in Table 1.

5. Summary

Grid-point temperatures from the ECHAM4/OPYC3 GSDIO integration were used as predictors for empirical downscaling of local monthly mean temperature over Norway during the period 1870-2050. The empirically downscaled temperature series indicate average annual warming rates of 0.2 to 0.5 °C per decade up to year 2050 at the Norwegian mainland, and 0.6 °C per decade on Svalbard. The warming rates are generally smallest in southern Norway along the west coast. They increase when moving inland and northwards. At the west coast in southern Norway, the modelled warming rates are rather similar in all seasons (0.2-0.3 °C per decade). Further north and in the inland, considerably larger warming rates are expected in winter than in summer. In Northern Norway and in inland valleys also in Southern Norway, winter warming rates of more than 0.5 °C per decade can be expected. At the Arctic stations the modelled winter warming rates are of magnitude 1 °C per decade.

The present results were compared to the results from dynamical downscaling. The results were rather similar in summer and autumn. In winter and spring, on the other hand, systematic differences were found: While the results were still quite similar at the west-coast of Southern Norway, the empirical downscaling gave larger warming rates in the inland, especially in valleys and other locations which are exposed for temperature inversions during winter. It is probably reasonable to expect larger winter warming in valleys than on mountains: The winter warming is probably accompanied by increased cyclonic activity, which leads to less favourable conditions for temperature inversions. Thus the empirical downscaling results may qualitatively be right on this point.

References

- Benestad, R.E., 2000: Future Climate Scenarios for Norway based on linear empirical downscaling and inferred directly from AOGCM results. DNMI Report 23/00 KLIMA, Norwegian Meteorological Institute, Oslo, Norway.
- Benestad, R.E., I. Hanssen-Bauer, I., E.J. Førland, O.E. Tveito and K. Iden, 1999: Evaluation of monthly mean data fields from the ECHAM4/OPYC3 control integration. DNMI Report 14/99 KLIMA, Norwegian Meteorological Institute, Oslo, Norway.
- Bjørge, D., J.E. Haugen and T.E. Nordeng, 2000: Future Climate in Norway. Dynamical downscaling experiments within the RegClim project. Research Report 103, Norwegian Meteorological Institute, Oslo, Norway.
- Førland, E.J., I.Hanssen-Bauer & P.Ø.Nordli, 1992: New Norwegian climate normals – but has the climate changed? *Norsk Geogr. Tidsskr.*, **46**, 83-94.
- Christensen, O.B., J.H. Christensen, B. Machenhauer & M. Botzet, 1998: Very high-resolution regional climate simulations over Scandinavia – Present climate. *J. Climate*, **11**, 3204-3229.
- Hanssen-Bauer, I., 2000: Evaluation and analysis of the ECHAM4/OPYC3 GSDIO temperature- and SLP-fields over Norway and Svalbard. DNMI Report 06/00 KLIMA, Norwegian Meteorological Institute, Oslo, Norway.
- Hanssen-Bauer, I. and E.J. Førland 1998: Long-term trends in precipitation and temperature in the Norwegian Arctic: can they be explained by changes in atmospheric circulation patterns? *Climate Research*, **10**, 143-153.
- Hanssen-Bauer, I. and E.J. Førland 2000a: Temperature and precipitation variations in Norway and their links to atmospheric circulation. *Int. J. Climatol*, **20**, No. 14, 1693-1708.
- Hanssen-Bauer, I. and E.J. Førland 2000b: Verification and analysis of a climate simulation of temperature and pressure fields over Norway and Svalbard. *Climate Research* (in press).
- Hanssen-Bauer, I. and P.Ø. Nordli 1998: Annual and seasonal temperature variations in Norway 1876-1997. DNMI Report 25/98 KLIMA, Norwegian Meteorological Institute, Oslo, Norway.
- Huth, R., J. Kysely & L. Pokorná, 2000: A GCM simulation of heat waves, dry spells, and their relationships to circulation. *Clim. Change*, **46**, 29-60.
- Iversen, T., E.J. Førland, L.P. Røed and F. Stordal, 1997: Regional Climate Under Global Warming. Project Description. NILU, P.O.Box 100, N-2007 Kjeller, Norway.
- Knippertz, P., U. Ulbrich and P. Speth, 2000: Changing cyclones and surface wind speeds over the North Atlantic and Europe in a transient GHG experiment. In press, *Climatic Research*
- Murphy J., 1999: An evaluation of statistical and dynamical techniques for downscaling local climate. *J. Climate*, **12**, 2256-2284.

- Roeckner, E., K. Arpe, L. Bengtsson, M. Christof, M. Claussen, L. Dümenil, M. Esch, M. Giorgetta, U. Schlese & U. Schulzweida, 1996: The atmospheric general circulation model ECHAM4: Model description and simulation of present-day climate. Report No. 218, Max-Planck-Institut für Meteorologie, Hamburg, Germany
- Roeckner, E., L. Bengtsson, J. Feichter, J. Lelieveld & H. Rohde, 1998: Transient climate change simulations with a coupled atmosphere-ocean GCM including the tropospheric sulphur cycle. Report No. 266, Max-Planck-Institut für Meteorologie, Hamburg, Germany
- Roeckner, E., L. Bengtsson, J. Feichter, J. Lelieveld & H. Rodhe, 1999: Transient climate change simulations with a coupled atmosphere-ocean GCM including the tropospheric sulphur cycle, *J.Climate*, **12**, 3004-3032.
- Skelly, W.C. & A. Henderson-Sellers, 1996: Grid box or grid point: What type of data do GCMs deliver to climate impact researchers? *Int. J. Climatol.* **16**, 1079-1086
- Singleton, F. & E. A. Spackman, 1984: Climatological network design. *Meteorol. Mag.* 113, 77-89.
- Zorita, E. and H. von Storch, 1999: A survey of statistical downscaling techniques. *J.Climate* (in press)
- Zorita, E., J.P. Hughes, D.P. Lettenmaier and H. von Storch, 1995: Stochastic Characterization of Regional Circulation Patterns for Climate Model Diagnosis and Estimation of Local Precipitation. *J.Climate*, **8**, 1023-1042.
- Werner P.C. and von Storch H., 1993: Interannual variability of Central Europe mean temperature in January-February and its relation to large-scale circulation. *Climate Research*, 3, 195-207
- Wilby R.L., L.E. Hay and G.H. Leavesley, 1999: A comparison of downscaled and raw GCM output: implications for climate change scenarios in the San Juan River basin, Colorado. *J. Hydrology*, 225 67-71

APPENDIX – 1

Table A1. Basic information for stations used in the present paper: Number and name, geographical coordinates, temperature region (Figure 1) and grid-point used for downscaling.

ST. NO.	STATION NAME	ALTITUDE	LATITUDE	LONGITUDE	REGION	GRID-POINT
6040	Flisa	184	60° 37'	12° 01'	1	1s
10400	Røros	628	62° 34'	11° 23'	1	1n
11500	Østre Toten	264	60° 42'	10° 52'	1	1s
12680	Lillehammer	270	61° 06'	10° 29'	1	1n
16610	Fokstua	972	62° 06'	9° 17'	1	1n
16740	Kjøremsgrendi	626	62° 06'	9° 03'	3	3
18700	Oslo-Blindern	94	59° 56'	10° 43'	1	1s
23160	Åbjørsbråten	639	60° 55'	9° 17'	1	1s
24880	Nesbyen	165	60° 34'	9° 08'	1	1s
25590	Geilo-Geilostølen	810	60° 31'	8° 12'	1	1s
27500	Færder Fyr	6	59° 01'	10° 31'	1	1s
31970	Gaustatoppen	1828	59° 51'	8° 40'	1	1s
32100	Gvarv	26	59° 23'	9° 11'	1	1s
37230	Tveitsund	252	59° 01'	8° 31'	1	1s
39100	Oksøy Fyr	9	58° 04'	8° 03'	1	1s
42160	Lista Fyr	14	58° 06'	6° 34'	1	1s
42920	Sirdal	500	58° 53'	6° 51'	2	2s
44560	Sola	7	58° 53'	5° 38'	2	2s
46610	Sauda	5	59° 38'	6° 21'	2	2s
47300	Utsira Fyr	55	59° 18'	4° 52'	2	2s
50540	Bergen-Florida	12	60° 23'	5° 20'	2	2s
51590	Voss-Bø	125	60° 38'	6° 29'	2	2s
52530	Hellisøy Fyr	20	60° 45'	4° 43'	2	2s
54130	Lærdal-Tønjum	36	61° 03'	7° 31'	2	2n
55840	Fjærland	10	61° 26'	6° 46'	2	2n
58700	Oppstryn	201	61° 56'	7° 13'	2	2n
59100	Kråkenes Fyr	41	62° 02'	4° 59'	2	2n
60500	Taffjord	15	62° 14'	7° 25'	2	2n
62480	Ona II	13	62° 52'	6° 32'	2	2n
69100	Værnes	12	63° 27'	10° 56'	3	3
70850	Kjøbli i Snåsa	195	64° 09'	12° 28'	3	3
71550	Ørland	10	63° 42'	9° 36'	3	3
75600	Leka	47	65° 05'	11° 42'	4	4s
77420	Majavatn	339	65° 10'	13° 25'	4	4s
80700	Glomfjord	39	66° 48'	13° 58'	4	4n
82290	Bodø	11	67° 16'	14° 26'	4	4n
85910	Røst II	10	67° 30'	12° 05'	4	4n
89950	Dividalen	228	68° 46'	19° 42'	5	5
90450	Tromsø	100	69° 39'	18° 55'	4	4n
92700	Loppa	10	70° 20'	21° 28'	4	4n
93300	Suolovuopmi	374	69° 35'	23° 31'	5	5
93900	Sihccajávri	382	68° 45'	23° 32'	5	5
96400	Sletnes	8	71° 05'	28° 13'	6	6
97250	Karasjok	129	69° 28'	25° 30'	5	5
98400	Makkaur	9	70° 42'	30° 04'	6	6
98550	Vardø	14	70° 22'	31° 05'	6	6
99710	Bjørnøya	16	74° 31'	19° 01'	A	A1
99720	Hopen	6	76° 30'	25° 04'	A	A2
99840	Svalbard Lufthavn	28	78° 15'	15° 28'	A	A3
99910	Ny-Ålesund	10	78° 55'	11° 56'	A	A3

APPENDIX – 2

Table A2 a) Observed and modelled mean values and standard deviations of monthly mean temperature (°C) at Røros during selected periods.

Monthly mean temperature (°C), 10400 Røros												
PERIOD	JAN	FEB	MAR	APR	MAY	JUN	JUL	AUG	SEP	OCT	NOV	DEC
O 1871-1900	-10.6	-10.8	-7.3	-1.5	4.0	9.6	11.3	9.9	6.0	0.3	-5.5	-9.9
B 1901-1930	-10.5	-9.4	-6.4	-1.5	4.2	8.5	11.4	9.6	5.6	0.2	-5.6	-9.1
S 1931-1960	-11.2	-9.9	-6.4	-0.7	5.0	9.4	12.5	10.9	6.6	1.1	-3.8	-7.4
1961-1990	-11.2	-9.7	-5.6	-0.7	5.6	10.1	11.4	10.4	6.1	1.7	-5.2	-9.1
M 1871-1900	-12.8	-10.4	-6.3	-0.9	5.7	10.3	11.3	10.2	6.2	1.7	-6.1	-9.6
1901-1930	-12.2	-10.9	-5.4	-1.3	5.3	9.7	11.0	9.9	6.1	1.3	-5.1	-9.3
O 1931-1960	-11.4	-9.5	-4.5	-0.8	5.0	10.1	11.0	9.8	5.6	1.1	-5.3	-8.8
D 1961-1990	-11.2	-9.7	-5.6	-0.7	5.6	10.1	11.4	10.4	6.1	1.7	-5.2	-9.1
2020-2049	-8.3	-6.7	-4.1	1.0	7.6	12.5	13.2	11.9	7.6	3.5	-3.1	-7.2
Standard deviation of monthly mean temperature (°C), 10400 Røros												
PERIOD	JAN	FEB	MAR	APR	MAY	JUN	JUL	AUG	SEP	OCT	NOV	DEC
O 1871-1900	4.1	4.7	2.8	2.1	1.8	1.4	1.3	1.2	1.2	2.1	2.6	3.5
B 1901-1930	3.3	3.1	2.9	1.9	1.7	1.7	2.0	1.4	0.9	2.2	2.4	3.5
S 1931-1960	4.1	4.5	3.3	1.5	1.6	1.7	1.3	1.5	1.3	1.7	2.1	2.7
1961-1990	4.9	4.2	2.9	1.6	1.3	1.6	1.2	1.2	1.3	1.5	2.7	4.0
M 1871-1900	4.5	4.2	2.7	1.4	2.0	2.0	1.9	1.2	1.4	1.7	2.7	3.2
1901-1930	5.0	5.0	3.2	1.9	1.9	1.8	1.7	1.1	1.2	1.8	2.7	4.2
O 1931-1960	3.7	3.5	2.5	1.4	1.6	1.3	1.6	1.3	1.4	2.1	2.7	2.5
D 1961-1990	3.0	4.0	2.9	1.9	1.7	1.9	1.6	1.3	1.2	2.2	2.2	3.1
2020-2049	3.6	3.0	3.0	1.7	1.9	1.6	2.3	1.1	1.1	1.8	2.0	3.4

Table A2 b) Observed and modelled mean values and standard deviations of monthly mean temperature (°C) at Oslo during selected periods.

Monthly mean temperature (°C), 18700 Oslo												
PERIOD	JAN	FEB	MAR	APR	MAY	JUN	JUL	AUG	SEP	OCT	NOV	DEC
O 1874-1900	-4.9	-4.6	-1.6	4.0	9.8	15.1	16.5	15.1	11.0	5.0	-0.2	-4.1
B 1901-1930	-4.1	-3.5	-0.5	4.4	10.0	14.3	16.9	14.9	10.8	5.4	0.0	-3.3
S 1931-1960	-4.7	-4.1	-0.5	4.8	10.7	14.7	17.3	16.0	11.3	5.9	1.1	-2.0
1961-1990	-4.3	-4.0	-0.2	4.5	10.8	15.2	16.4	15.2	10.8	6.3	0.7	-3.1
M 1874-1900	-5.6	-4.1	-0.8	4.5	10.9	15.5	16.5	15.0	10.8	6.1	0.4	-3.4
1901-1930	-4.7	-4.6	-0.2	3.9	10.5	14.9	16.2	14.8	10.9	6.1	0.6	-3.3
O 1931-1960	-4.4	-3.8	0.5	4.5	10.3	15.6	16.1	14.6	10.5	5.9	0.7	-2.7
D 1961-1990	-4.3	-4.0	-0.2	4.5	10.8	15.2	16.4	15.2	10.8	6.3	0.7	-3.1
2020-2049	-1.8	-1.3	1.4	6.3	12.3	17.3	17.8	16.4	12.1	8.0	2.8	-1.6
Standard deviation of monthly mean temperature (°C), 18700 Oslo												
PERIOD	JAN	FEB	MAR	APR	MAY	JUN	JUL	AUG	SEP	OCT	NOV	DEC
O 1874-1900	2.8	3.0	2.3	1.4	1.8	1.4	1.2	1.4	1.1	1.7	1.8	2.4
B 1901-1930	2.6	2.5	1.9	1.4	1.5	1.5	1.8	1.2	0.9	1.8	1.8	2.8
S 1931-1960	2.9	3.3	2.3	1.2	1.4	1.5	1.3	1.7	1.3	1.4	1.6	2.1
1961-1990	3.5	3.5	2.2	1.3	1.2	1.5	1.2	1.4	1.1	1.3	1.8	2.7
M 1874-1900	3.2	3.0	2.3	1.3	1.5	1.7	1.5	0.9	1.0	1.4	2.3	2.5
1901-1930	3.5	3.8	2.9	1.9	1.7	1.4	1.7	1.0	1.0	1.5	2.7	3.0
O 1931-1960	2.7	3.0	2.2	1.5	1.4	1.3	1.5	1.0	1.0	1.8	2.4	1.5
D 1961-1990	2.3	3.4	2.7	2.0	1.5	1.5	1.3	1.4	0.9	1.9	2.1	2.2
2020-2049	2.7	2.6	2.7	1.9	1.8	1.3	1.9	1.0	0.9	1.4	1.9	2.8

APPENDIX – 2

Table A2 c) Observed and modelled mean values and standard deviations of monthly mean temperature (°C) at Nesbyen during selected periods.

Monthly mean temperature (°C), 24880 Nesbyen													
PERIOD	JAN	FEB	MAR	APR	MAY	JUN	JUL	AUG	SEP	OCT	NOV	DEC	
O 1901-1930	-10.0	-7.7	-2.6	2.7	8.3	13.0	15.4	12.9	8.4	2.5	-4.2	-9.5	
B 1931-1960	-10.8	-8.7	-3.1	3.3	9.0	13.6	15.8	13.9	8.9	3.2	-2.8	-7.2	
S 1961-1990	-10.5	-8.6	-2.3	3.0	9.1	14.1	15.2	13.5	8.6	3.6	-4.0	-8.6	
M 1901-1930	-11.1	-9.5	-2.3	2.5	8.9	13.9	15.1	13.2	8.7	3.3	-4.1	-8.9	
O 1931-1960	-10.7	-8.4	-1.5	3.0	8.6	14.5	14.9	12.9	8.3	3.2	-4.1	-8.0	
D 1961-1990	-10.5	-8.6	-2.3	3.0	9.1	14.1	15.2	13.5	8.6	3.6	-4.0	-8.6	
<i>2020-2049</i>	<i>-6.8</i>	<i>-4.4</i>	<i>-0.4</i>	<i>4.6</i>	<i>10.5</i>	<i>16.0</i>	<i>16.5</i>	<i>14.6</i>	<i>9.8</i>	<i>5.5</i>	<i>-1.3</i>	<i>-6.3</i>	
Standard deviation of monthly mean temperature (°C), 24880 Nesbyen													
PERIOD	JAN	FEB	MAR	APR	MAY	JUN	JUL	AUG	SEP	OCT	NOV	DEC	
O 1901-1930	4.1	3.5	2.5	1.4	1.3	1.4	1.5	1.2	1.0	2.1	2.6	4.1	
B 1931-1960	4.2	4.4	3.1	1.5	1.2	1.3	1.2	1.5	1.3	1.6	2.4	3.1	
S 1961-1990	4.9	4.4	2.9	1.3	1.1	1.5	1.2	1.3	1.2	1.5	3.0	3.8	
M 1901-1930	5.4	5.8	3.5	1.8	1.6	1.3	1.5	0.9	0.9	1.6	3.5	4.5	
O 1931-1960	4.1	4.6	2.6	1.4	1.3	1.2	1.3	0.9	0.9	2.0	3.1	2.4	
D 1961-1990	3.5	5.2	3.2	1.8	1.4	1.3	1.2	1.2	0.8	2.1	2.7	3.4	
<i>2020-2049</i>	<i>4.1</i>	<i>4.0</i>	<i>3.3</i>	<i>1.8</i>	<i>1.7</i>	<i>1.2</i>	<i>1.8</i>	<i>0.9</i>	<i>0.8</i>	<i>1.5</i>	<i>2.4</i>	<i>4.3</i>	

Table A2 d) Observed and modelled mean values and standard deviations of monthly mean temperature (°C) at Oksøy during selected periods.

Monthly mean temperature (°C), 39100 Oksøy													
PERIOD	JAN	FEB	MAR	APR	MAY	JUN	JUL	AUG	SEP	OCT	NOV	DEC	
O 1875-1900	0.2	-0.2	0.7	4.3	9.0	13.2	15.3	15.0	12.6	8.0	4.4	1.6	
B 1901-1930	1.0	0.4	1.5	4.6	8.9	12.7	15.5	14.7	12.3	8.4	4.5	2.0	
S 1931-1960	0.2	-0.3	1.2	4.9	9.5	13.0	16.0	15.7	13.1	9.1	5.4	2.8	
S 1961-1990	0.3	-0.3	1.6	4.5	9.3	13.3	15.2	15.2	12.5	9.3	5.0	2.1	
M 1875-1900	-0.8	-0.3	1.0	4.4	9.4	13.5	15.3	15.0	12.5	9.1	4.8	2.0	
M 1901-1930	0.0	-0.8	1.6	4.0	9.1	13.1	15.1	14.9	12.6	9.1	5.0	1.9	
O 1931-1960	0.2	-0.2	2.2	4.5	8.9	13.7	14.9	14.7	12.3	9.0	5.0	2.4	
D 1961-1990	0.3	-0.3	1.6	4.5	9.3	13.3	15.2	15.2	12.5	9.3	5.0	2.1	
<i>2020-2049</i>	<i>2.4</i>	<i>2.0</i>	<i>2.9</i>	<i>5.9</i>	<i>10.6</i>	<i>15.0</i>	<i>16.4</i>	<i>16.2</i>	<i>13.6</i>	<i>10.7</i>	<i>6.8</i>	<i>3.4</i>	
Standard deviation of monthly mean temperature (°C), 39100 Oksøy													
PERIOD	JAN	FEB	MAR	APR	MAY	JUN	JUL	AUG	SEP	OCT	NOV	DEC	
O 1875-1900	2.4	2.8	1.9	1.2	1.4	1.1	1.0	1.1	1.0	1.3	1.6	2.0	
B 1901-1930	1.9	2.2	1.7	1.1	1.2	1.3	1.4	1.2	0.8	1.3	1.7	2.2	
S 1931-1960	2.5	3.1	2.2	1.2	1.0	1.2	1.0	1.3	1.0	1.3	1.3	1.7	
S 1961-1990	3.1	3.0	2.0	1.1	1.0	1.1	1.0	1.1	0.8	1.0	1.5	2.3	
M 1875-1900	2.8	2.6	1.9	1.1	1.3	1.3	1.2	0.7	0.8	1.2	2.0	2.2	
M 1901-1930	3.0	3.2	2.5	1.6	1.4	1.2	1.4	0.9	0.9	1.3	2.3	2.5	
O 1931-1960	2.3	2.6	1.9	1.3	1.1	1.1	1.2	0.8	0.8	1.5	2.0	1.3	
D 1961-1990	1.9	2.9	2.3	1.6	1.2	1.2	1.1	1.1	0.7	1.6	1.8	1.9	
<i>2020-2049</i>	<i>2.3</i>	<i>2.2</i>	<i>2.3</i>	<i>1.6</i>	<i>1.5</i>	<i>1.1</i>	<i>1.6</i>	<i>0.8</i>	<i>0.7</i>	<i>1.2</i>	<i>1.6</i>	<i>2.4</i>	

APPENDIX – 2

Table A2 e) Observed and modelled mean values and standard deviations of monthly mean temperature (°C) at Bergen during selected periods.

Monthly mean temperature (°C), 50540 Bergen												
PERIOD	JAN	FEB	MAR	APR	MAY	JUN	JUL	AUG	SEP	OCT	NOV	DEC
O 1874-1900	1.3	1.0	2.1	5.6	9.3	13.1	14.5	13.9	11.1	7.2	4.1	1.7
B 1901-1930	1.6	1.7	2.9	6.0	9.5	12.3	14.4	13.5	10.9	7.6	4.0	2.4
S 1931-1960	1.1	1.2	3.2	6.1	10.5	12.9	15.3	14.7	11.8	8.1	5.3	3.0
1961-1990	1.3	1.5	3.3	5.9	10.5	13.3	14.3	14.1	11.2	8.6	4.6	2.4
M 1874-1900	0.4	1.3	2.6	5.9	10.5	13.7	14.5	14.0	11.3	8.6	4.2	2.0
O 1901-1930	0.9	1.4	3.3	5.6	10.3	12.6	14.3	13.7	11.3	8.4	4.4	2.0
D 1931-1960	1.2	1.6	4.2	6.0	9.8	13.7	14.3	13.7	11.1	8.4	4.4	2.5
1961-1990	1.3	1.5	3.3	5.9	10.5	13.3	14.3	14.1	11.2	8.6	4.6	2.4
2020-2049	3.3	3.6	4.9	7.8	12.0	15.4	15.9	15.5	12.7	10.4	6.5	3.5
Standard deviation of monthly mean temperature (°C), 50540 Bergen												
PERIOD	JAN	FEB	MAR	APR	MAY	JUN	JUL	AUG	SEP	OCT	NOV	DEC
O 1874-1900	2.1	2.2	1.6	1.3	1.6	1.3	1.3	1.1	1.1	1.5	1.7	2.2
B 1901-1930	1.7	1.6	1.6	1.5	1.4	1.6	1.7	1.5	1.0	1.4	1.6	1.9
S 1931-1960	2.3	2.2	1.9	1.0	1.4	1.6	1.0	1.2	1.4	1.2	1.4	1.5
1961-1990	2.7	2.2	1.4	1.0	1.1	1.3	1.0	1.1	1.2	1.1	1.5	2.0
M 1874-1900	1.9	2.0	1.7	1.1	1.6	2.0	1.8	1.0	0.9	1.2	2.0	1.8
O 1901-1930	2.3	2.2	2.2	1.6	1.4	1.4	1.6	1.1	0.9	1.4	2.5	2.3
D 1931-1960	1.9	1.7	1.6	1.3	1.3	1.6	1.6	1.0	1.1	1.6	2.2	1.3
1961-1990	1.6	2.2	2.2	1.7	1.4	1.5	1.3	1.1	1.0	1.7	1.8	1.6
2020-2049	1.9	1.9	2.0	1.5	1.5	1.5	1.7	1.0	0.9	1.2	1.7	2.4

Table A2 f) Observed and modelled mean values and standard deviations of monthly mean temperature (°C) at Værnes during selected periods.

Monthly mean temperature (°C), 69100 Værnes												
PERIOD	JAN	FEB	MAR	APR	MAY	JUN	JUL	AUG	SEP	OCT	NOV	DEC
O 1871-1900	-3.0	-3.1	-0.8	3.8	7.9	12.2	14.2	13.1	9.7	4.6	0.7	-2.4
B 1901-1930	-2.8	-2.2	0.1	4.0	8.2	11.6	14.3	13.1	9.5	4.6	0.5	-1.6
S 1931-1960	-3.6	-2.9	-0.3	3.9	8.5	11.8	14.9	13.8	10.1	5.2	1.6	-0.9
1961-1990	-3.4	-2.5	0.1	3.6	9.1	12.5	13.7	13.3	9.5	5.7	0.5	-1.7
M 1871-1900	-4.6	-3.0	-0.4	3.5	9.1	12.6	13.7	13.3	9.6	5.7	-0.2	-2.1
O 1901-1930	-4.1	-3.3	0.2	3.2	9.0	12.1	13.5	12.9	9.5	5.4	0.4	-1.9
D 1931-1960	-3.3	-2.5	1.2	3.6	8.7	12.4	13.6	13.0	9.1	5.3	0.4	-1.5
1961-1990	-3.4	-2.5	0.1	3.6	9.1	12.5	13.7	13.3	9.5	5.7	0.5	-1.7
2020-2049	-1.1	-0.3	1.4	5.0	10.7	14.4	15.2	14.5	10.7	7.4	2.1	-0.1
Standard deviation of monthly mean temperature (°C), 69100 Værnes												
PERIOD	JAN	FEB	MAR	APR	MAY	JUN	JUL	AUG	SEP	OCT	NOV	DEC
O 1871-1900	3.0	3.5	2.1	1.6	1.5	1.5	1.3	1.2	1.2	1.7	1.9	2.7
B 1901-1930	1.9	1.8	2.0	1.4	1.5	1.7	2.0	1.6	0.9	1.7	1.8	2.6
S 1931-1960	2.8	3.2	2.6	1.3	1.6	1.7	1.4	1.5	1.3	1.6	1.6	2.0
1961-1990	3.5	3.3	2.0	1.4	1.4	1.5	1.1	1.2	1.5	1.5	2.0	3.0
M 1871-1900	3.0	2.9	1.8	0.9	1.2	1.4	1.3	1.0	1.0	1.2	2.1	2.3
O 1901-1930	3.4	3.5	2.4	1.4	1.3	1.4	1.3	0.9	0.9	1.4	2.2	2.9
D 1931-1960	2.5	2.7	1.7	1.0	1.3	1.1	1.4	1.2	1.2	1.7	2.1	1.6
1961-1990	2.3	2.9	2.4	1.5	1.3	1.7	1.3	1.1	1.0	1.8	1.3	2.3
2020-2049	2.3	2.1	2.1	1.3	1.4	1.4	1.8	1.0	0.8	1.4	1.6	2.2

APPENDIX – 2

Table A2 g) Observed and modelled mean values and standard deviations of monthly mean temperature (°C) at Bodø during selected periods.

Monthly mean temperature (°C), 82290 Bodø												
PERIOD	JAN	FEB	MAR	APR	MAY	JUN	JUL	AUG	SEP	OCT	NOV	DEC
O 1871-1900	-1.7	-2.4	-1.6	1.9	5.9	10.0	12.6	12.0	8.7	4.4	1.2	-1.3
B 1901-1930	-1.1	-1.8	-0.8	2.4	6.2	9.6	12.8	12.6	8.8	4.3	0.8	-1.3
S 1931-1960	-2.1	-2.4	-1.0	2.3	6.4	10.0	13.7	12.7	9.3	5.0	1.9	-0.1
1961-1990	-2.2	-2.0	-0.6	2.5	7.2	10.4	12.5	12.3	9.0	5.3	1.2	-1.2
M 1871-1900	-3.0	-2.6	-1.1	2.4	7.2	10.3	12.2	12.5	9.1	5.0	0.3	-1.6
O 1901-1930	-2.8	-2.1	-0.2	2.4	7.6	10.4	12.2	12.0	8.8	5.3	0.9	-0.9
D 1931-1960	-2.7	-2.6	0.5	2.3	7.1	10.1	12.4	12.2	8.4	4.8	1.2	-1.1
1961-1990	-2.2	-2.0	-0.6	2.5	7.2	10.4	12.5	12.3	9.0	5.3	1.2	-1.2
2020-2049	0.5	0.9	2.1	4.4	10.3	12.8	14.6	14.4	11.1	8.1	3.6	1.0
Standard deviation of monthly mean temperature (°C), 82290 Bodø												
PERIOD	JAN	FEB	MAR	APR	MAY	JUN	JUL	AUG	SEP	OCT	NOV	DEC
O 1871-1900	2.2	2.8	2.0	1.8	1.6	1.8	1.5	1.5	1.5	1.9	1.8	2.2
B 1901-1930	1.9	1.8	2.0	1.5	1.3	1.4	1.9	1.4	1.1	1.9	1.9	2.3
S 1931-1960	2.1	2.6	2.0	1.5	1.5	1.5	1.7	1.6	1.4	1.7	1.6	2.1
1961-1990	2.1	2.6	1.7	1.3	1.5	1.6	1.5	1.3	1.3	1.7	1.6	2.5
M 1871-1900	2.6	2.8	1.3	1.4	1.4	1.3	1.1	1.3	1.9	1.5	2.3	2.3
O 1901-1930	2.5	2.9	2.4	1.5	1.2	1.3	1.3	1.5	1.4	1.9	2.2	2.4
D 1931-1960	2.6	2.3	2.6	1.0	1.4	1.4	1.5	1.6	1.8	2.0	2.4	2.5
1961-1990	2.5	1.7	2.2	1.4	1.1	1.2	1.2	1.4	1.3	2.3	1.7	2.4
2020-2049	2.3	1.8	1.6	1.1	1.3	1.1	1.1	1.2	1.3	1.9	1.7	2.1

Table A2 h) Observed and modelled mean values and standard deviations of monthly mean temperature (°C) at Tromsø during selected periods.

Monthly mean temperature (°C), 90450 Tromsø												
PERIOD	JAN	FEB	MAR	APR	MAY	JUN	JUL	AUG	SEP	OCT	NOV	DEC
O 1871-1900	-3.3	-4.1	-3.6	-0.4	3.2	7.7	10.5	9.8	6.4	2.1	-0.8	-3.1
B 1901-1930	-3.1	-3.8	-3.1	-0.1	3.3	7.8	11.1	10.5	6.6	2.0	-1.1	-3.0
S 1931-1960	-3.5	-4.0	-2.7	0.3	4.1	8.8	12.4	11.1	7.3	3.0	-0.1	-1.9
1961-1990	-4.4	-4.2	-2.7	0.3	4.8	9.1	11.8	10.8	6.7	2.7	-1.1	-3.3
M 1871-1900	-5.3	-4.9	-3.2	0.2	4.8	9.0	11.5	10.9	6.8	2.5	-2.0	-3.8
O 1901-1930	-5.1	-4.3	-2.3	0.2	5.2	9.1	11.6	10.6	6.5	2.7	-1.4	-3.0
D 1931-1960	-4.9	-4.9	-1.5	0.1	4.7	8.9	11.7	10.7	6.2	2.2	-1.1	-3.2
1961-1990	-4.4	-4.2	-2.7	0.3	4.8	9.1	11.8	10.8	6.7	2.7	-1.1	-3.3
2020-2049	-1.4	-1.0	0.1	2.2	7.6	11.0	13.4	12.4	8.4	5.1	1.3	-0.8
Standard deviation of monthly mean temperature (°C), 90450 Tromsø												
PERIOD	JAN	FEB	MAR	APR	MAY	JUN	JUL	AUG	SEP	OCT	NOV	DEC
O 1871-1900	2.0	2.5	1.8	1.7	1.6	1.8	1.3	1.1	1.4	1.7	1.5	2.0
B 1901-1930	1.9	1.9	1.9	1.5	1.5	1.6	1.8	1.3	1.1	2.0	1.8	2.1
S 1931-1960	1.8	2.2	1.6	1.4	1.4	1.6	1.8	1.4	1.4	1.8	1.6	2.1
1961-1990	1.9	2.2	1.9	1.3	1.6	1.8	1.8	1.2	1.4	1.8	1.6	2.3
M 1871-1900	2.9	3.1	1.4	1.4	1.2	1.0	0.9	1.0	1.6	1.3	2.2	2.6
O 1901-1930	2.7	3.2	2.5	1.6	1.1	1.0	1.0	1.1	1.1	1.7	2.2	2.7
D 1931-1960	2.9	2.5	2.8	1.0	1.3	1.1	1.2	1.3	1.4	1.7	2.3	2.8
1961-1990	2.8	1.9	2.3	1.4	1.0	1.0	1.0	1.1	1.1	2.0	1.7	2.7
2020-2049	2.5	2.0	1.7	1.1	1.2	0.9	0.9	0.9	1.1	1.6	1.6	2.3

APPENDIX – 2

Table A2 i) Observed and modelled mean values and standard deviations of monthly mean temperature (°C) at Karasjok during selected periods.

Monthly mean temperature (°C), 97250 Karasjok													
	PERIOD	JAN	FEB	MAR	APR	MAY	JUN	JUL	AUG	SEP	OCT	NOV	DEC
OBSERVED	1876-1900	-15.5	-14.6	-11.3	-3.9	3.2	9.3	12.4	10.4	5.0	-2.2	-9.6	-14.9
	1901-1930	-14.3	-14.7	-10.0	-3.3	3.2	9.5	13.2	10.5	5.6	-2.1	-9.6	-13.2
	1931-1960	-14.9	-14.6	-10.1	-3.2	3.6	9.9	13.7	11.3	5.9	-1.3	-7.3	-11.9
	1961-1990	-17.1	-15.4	-10.3	-3.1	3.8	10.1	13.1	10.7	5.3	-1.3	-9.4	-15.3
MODELLED	1876-1900	-17.4	-15.4	-10.9	-3.0	4.3	10.6	12.9	11.0	5.2	-1.8	-10.1	-15.4
	1901-1930	-17.6	-15.0	-9.4	-3.4	4.4	10.5	12.3	10.1	5.4	-0.8	-8.5	-14.3
	1931-1960	-17.6	-16.1	-8.9	-3.7	3.6	9.7	12.4	10.3	5.1	-1.8	-8.7	-14.2
	1961-1990	-17.1	-15.4	-10.3	-3.1	3.8	10.1	13.1	10.7	5.3	-1.3	-9.4	-15.3
	2020-2049	-11.9	-10.5	-7.5	-1.6	7.4	13.0	14.9	11.9	6.8	1.5	-5.0	-11.3
Standard deviation of monthly mean temperature (°C), 97250 Karasjok													
	PERIOD	JAN	FEB	MAR	APR	MAY	JUN	JUL	AUG	SEP	OCT	NOV	DEC
OBSERVED	1876-1900	4.7	5.4	3.6	2.3	2.4	2.5	1.6	1.5	2.7	3.1	3.5	4.7
	1901-1930	4.1	3.9	3.8	2.1	1.7	1.8	2.1	1.2	1.2	2.9	3.8	4.5
	1931-1960	4.2	4.6	2.8	2.1	1.9	2.1	1.9	1.6	1.4	2.2	3.3	4.8
	1961-1990	4.4	5.1	3.8	1.9	1.9	2.0	1.8	1.2	1.5	2.7	3.7	5.3
MODELLED	1876-1900	5.7	5.0	2.9	1.3	1.9	1.9	2.3	1.6	1.9	1.8	3.7	4.2
	1901-1930	5.4	5.8	4.0	2.0	1.3	1.9	2.2	1.5	1.2	2.0	3.5	4.7
	1931-1960	4.6	4.4	3.8	1.1	1.3	2.0	2.2	2.0	1.6	2.1	3.4	3.6
	1961-1990	4.7	3.3	3.6	1.9	1.7	2.2	2.3	1.5	1.2	2.7	3.1	4.9
	2020-2049	4.9	4.1	2.8	1.1	2.0	1.9	2.7	1.3	1.5	1.9	2.1	4.2

Table A2 j) Observed and modelled mean values and standard deviations of monthly mean temperature (°C) at Vardø during selected periods.

Monthly mean temperature (°C), 98550 Vardø													
	PERIOD	JAN	FEB	MAR	APR	MAY	JUN	JUL	AUG	SEP	OCT	NOV	DEC
OBSERVED	1871-1900	-5.4	-5.6	-4.8	-1.6	1.5	5.2	8.2	8.5	6.2	1.7	-2.1	-4.6
	1901-1930	-4.9	-5.4	-4.1	-1.3	2.0	5.8	8.9	8.8	6.5	1.7	-1.6	-3.6
	1931-1960	-4.3	-5.2	-4.0	-0.8	2.6	6.2	9.1	9.7	6.8	2.5	-0.5	-2.7
	1961-1990	-5.1	-5.4	-3.6	-1.1	2.5	6.2	9.2	9.1	6.6	2.4	-1.3	-3.7
MODELLED	1871-1900	-4.8	-5.4	-3.4	-1.1	2.7	6.6	9.3	9.3	6.8	2.4	-1.3	-3.6
	1901-1930	-4.3	-4.3	-2.5	-0.7	3.1	6.6	9.1	8.9	6.7	3.2	-0.3	-2.6
	1931-1960	-4.7	-5.1	-3.1	-1.4	2.6	6.2	9.0	8.9	6.8	2.7	-0.4	-2.8
	1961-1990	-5.1	-5.4	-3.6	-1.1	2.5	6.2	9.2	9.1	6.6	2.4	-1.3	-3.7
	2020-2049	-1.5	-2.0	-0.6	1.0	5.0	8.3	10.7	10.3	8.1	5.2	2.1	-0.3
Standard deviation of monthly mean temperature (°C), 98550 Vardø													
	PERIOD	JAN	FEB	MAR	APR	MAY	JUN	JUL	AUG	SEP	OCT	NOV	DEC
OBSERVED	1871-1900	1.7	2.0	1.8	1.7	1.7	1.3	1.2	1.2	1.4	1.4	1.5	1.7
	1901-1930	2.0	1.9	1.7	1.5	1.4	1.2	1.2	1.2	1.1	1.7	1.4	1.7
	1931-1960	1.4	1.9	1.6	1.3	1.2	1.1	1.5	1.1	1.1	1.3	1.3	2.1
	1961-1990	1.4	2.1	2.0	1.4	1.2	1.3	1.4	1.1	1.1	1.5	1.5	1.7
MODELLED	1871-1900	1.8	2.1	1.2	1.0	1.0	1.2	1.4	1.3	1.5	1.1	1.4	1.4
	1901-1930	1.9	1.6	1.4	1.2	1.0	0.9	1.1	1.2	0.8	1.3	1.7	1.7
	1931-1960	1.8	2.0	2.3	1.5	1.0	1.1	1.5	1.6	1.3	1.3	1.4	1.6
	1961-1990	2.1	1.8	1.5	1.0	1.0	1.2	1.9	1.8	1.0	1.4	1.5	1.8
	2020-2049	1.6	1.3	0.9	0.8	0.8	0.9	1.4	1.0	1.0	1.0	1.1	1.4

APPENDIX – 2

Table A2 k) Observed and modelled mean values and standard deviations of monthly mean temperature (°C) at Bjørnøya during selected periods.

Monthly mean temperature (°C), 99710 Bjørnøya												
PERIOD	JAN	FEB	MAR	APR	MAY	JUN	JUL	AUG	SEP	OCT	NOV	DEC
O 1931-1960	-5.7	-6.9	-7.2	-5.4	-1.3	2.0	4.5	5.0	3.0	0.4	-2.0	-3.9
B 1961-1990	-8.1	-7.7	-7.6	-5.4	-1.4	1.8	4.4	4.4	2.7	-0.5	-3.7	-7.1
M 1931-1960	-7.0	-7.2	-6.3	-5.3	-1.1	2.1	4.9	4.8	3.0	0.0	-3.0	-5.7
O 1961-1990	-8.1	-7.7	-7.6	-5.4	-1.4	1.8	4.4	4.4	2.7	-0.5	-3.7	-7.1
D 2020-2049	-3.0	-2.7	-2.8	-1.5	0.8	4.4	6.7	6.5	4.6	2.6	0.6	-2.3
Standard deviation of monthly mean temperature (°C), 99710 Bjørnøya												
PERIOD	JAN	FEB	MAR	APR	MAY	JUN	JUL	AUG	SEP	OCT	NOV	DEC
O 1931-1960	3.5	3.3	3.2	2.4	1.5	1.1	1.1	1.0	1.2	1.3	2.2	2.9
B 1961-1990	3.8	4.0	4.1	2.3	1.4	1.2	1.2	1.0	1.2	2.1	2.7	3.7
M 1931-1960	4.0	4.2	4.4	3.9	1.2	1.1	1.4	1.5	1.5	2.2	3.3	3.7
O 1961-1990	3.9	4.6	3.5	3.3	1.2	0.9	1.2	1.3	1.2	1.9	3.5	3.4
D 2020-2049	1.2	1.1	1.3	1.3	0.7	0.9	0.6	0.7	0.9	1.0	1.3	1.2

Table A2 l) Observed and modelled mean values and standard deviations of monthly mean temperature (°C) at Svalbard Airport during selected periods.

Monthly mean temperature (°C), 99840 Svalbard Airport												
PERIOD	JAN	FEB	MAR	APR	MAY	JUN	JUL	AUG	SEP	OCT	NOV	DEC
O 1912-1930	-16.1	-17.3	-18.8	-13.8	-5.1	2.6	5.6	4.4	-0.3	-6.1	-11.1	-12.7
B 1931-1960	-12.4	-13.6	-14.9	-11.3	-3.8	2.3	5.9	4.6	0.7	-4.4	-7.8	-10.1
S 1961-1990	-15.3	-16.2	-15.7	-12.2	-4.1	2.0	5.9	4.7	0.3	-5.5	-10.3	-13.4
M 1912-1930	-14.4	-15.5	-15.6	-12.1	-4.2	2.3	5.9	4.7	0.4	-5.3	-9.4	-12.0
O 1931-1960	-13.9	-16.7	-14.9	-13.1	-4.3	2.0	6.1	5.0	0.5	-4.7	-9.7	-11.4
D 1961-1990	-15.3	-16.2	-15.7	-12.2	-4.1	2.0	5.9	4.7	0.3	-5.5	-10.3	-13.4
2020-2049	-8.6	-11.9	-10.6	-9.2	-2.8	3.6	7.7	6.6	2.2	-1.8	-4.6	-6.7
Standard deviation of monthly mean temperature (°C), 99840 Svalbard Airport												
PERIOD	JAN	FEB	MAR	APR	MAY	JUN	JUL	AUG	SEP	OCT	NOV	DEC
O 1912-1930	6.2	5.9	4.6	4.0	2.1	1.1	1.3	1.1	1.4	1.9	3.8	5.0
B 1931-1960	4.4	3.2	3.4	2.5	1.6	0.7	0.7	0.8	1.4	2.2	3.4	3.7
S 1961-1990	5.1	4.0	4.2	2.9	1.5	1.2	0.9	0.7	1.6	2.9	3.7	4.7
M 1912-1930	5.2	4.3	4.4	3.2	1.7	1.0	1.0	0.8	1.5	2.4	3.9	4.4
O 1931-1960	4.3	4.6	4.7	4.9	0.9	0.7	1.1	1.2	1.2	2.0	4.1	4.1
D 1961-1990	4.9	4.7	4.4	3.9	0.9	0.8	1.1	1.1	1.5	2.3	3.9	4.7
2020-2049	3.5	3.0	3.6	3.5	1.0	1.4	1.3	1.3	1.3	1.9	2.9	3.0

APPENDIX – 3

Table A3. Seasonal/annual temperature increase ($^{\circ}\text{C}$ per decade) from 1961-90 to 2021-50, with 95% confidence intervals.

	WIN	SPR	SUM	AUT	ANNUAL
6040 Flisa	0.53 ± 0.24	0.29 ± 0.15	0.26 ± 0.09	0.33 ± 0.12	0.35 ± 0.09
10400 Røros	0.44 ± 0.20	0.28 ± 0.14	0.31 ± 0.11	0.31 ± 0.12	0.33 ± 0.09
11500 Østre Toten	0.44 ± 0.20	0.28 ± 0.15	0.27 ± 0.10	0.30 ± 0.11	0.32 ± 0.09
12680 Lillehammer	0.40 ± 0.18	0.29 ± 0.15	0.29 ± 0.10	0.31 ± 0.11	0.32 ± 0.08
16610 Fokstua	0.30 ± 0.13	0.27 ± 0.13	0.31 ± 0.11	0.27 ± 0.10	0.29 ± 0.07
16740 Kjøremsgrendi	0.36 ± 0.16	0.26 ± 0.13	0.29 ± 0.10	0.27 ± 0.10	0.29 ± 0.07
18700 Oslo	0.37 ± 0.17	0.27 ± 0.14	0.26 ± 0.09	0.28 ± 0.10	0.30 ± 0.08
23160 Åbjørsbråten	0.41 ± 0.19	0.28 ± 0.15	0.27 ± 0.10	0.30 ± 0.10	0.31 ± 0.08
24880 Nesbyen	0.57 ± 0.18	0.27 ± 0.15	0.24 ± 0.10	0.32 ± 0.10	0.35 ± 0.08
25590 Geilo	0.40 ± 0.25	0.28 ± 0.15	0.27 ± 0.09	0.30 ± 0.11	0.31 ± 0.09
27500 Færder Fyr	0.33 ± 0.15	0.24 ± 0.12	0.23 ± 0.08	0.25 ± 0.09	0.27 ± 0.07
31970 Gaustatoppen	0.31 ± 0.14	0.28 ± 0.14	0.29 ± 0.10	0.28 ± 0.10	0.29 ± 0.08
32100 Gvarv	0.42 ± 0.19	0.26 ± 0.14	0.24 ± 0.09	0.28 ± 0.10	0.30 ± 0.08
37230 Tveitsund	0.43 ± 0.19	0.27 ± 0.14	0.26 ± 0.09	0.30 ± 0.10	0.31 ± 0.08
39100 Oksøy Fyr	0.32 ± 0.14	0.22 ± 0.12	0.22 ± 0.08	0.24 ± 0.08	0.25 ± 0.07
42160 Lista Fyr	0.30 ± 0.13	0.22 ± 0.11	0.22 ± 0.08	0.23 ± 0.08	0.24 ± 0.06
42920 Sirdal	0.41 ± 0.17	0.29 ± 0.11	0.28 ± 0.09	0.33 ± 0.11	0.33 ± 0.07
44560 Sola	0.33 ± 0.14	0.27 ± 0.10	0.27 ± 0.09	0.30 ± 0.09	0.29 ± 0.07
46610 Sauda	0.36 ± 0.15	0.30 ± 0.12	0.30 ± 0.10	0.33 ± 0.11	0.32 ± 0.07
47300 Utsira Fyr	0.23 ± 0.10	0.23 ± 0.09	0.23 ± 0.08	0.24 ± 0.08	0.23 ± 0.05
50540 Bergen	0.28 ± 0.12	0.28 ± 0.11	0.28 ± 0.09	0.29 ± 0.09	0.28 ± 0.06
51590 Voss	0.47 ± 0.20	0.33 ± 0.13	0.31 ± 0.10	0.37 ± 0.12	0.37 ± 0.08
52530 Hellisøy Fyr	0.23 ± 0.10	0.23 ± 0.09	0.23 ± 0.08	0.24 ± 0.08	0.23 ± 0.05
54130 Lærdal	0.40 ± 0.16	0.28 ± 0.11	0.27 ± 0.09	0.32 ± 0.10	0.32 ± 0.07
55840 Fjærland	0.42 ± 0.15	0.32 ± 0.11	0.34 ± 0.10	0.37 ± 0.12	0.36 ± 0.07
58700 Oppstryn	0.32 ± 0.11	0.35 ± 0.11	0.39 ± 0.11	0.38 ± 0.12	0.36 ± 0.07
59100 Kråkenes Fyr	0.23 ± 0.08	0.26 ± 0.08	0.29 ± 0.08	0.28 ± 0.09	0.26 ± 0.05
60500 Tafjord	0.34 ± 0.12	0.31 ± 0.10	0.34 ± 0.10	0.35 ± 0.11	0.34 ± 0.06
62480 Ona	0.23 ± 0.08	0.23 ± 0.08	0.26 ± 0.07	0.26 ± 0.08	0.25 ± 0.05
69100 Værnes	0.34 ± 0.14	0.24 ± 0.11	0.25 ± 0.09	0.25 ± 0.09	0.27 ± 0.07
70850 Kjøbli i Snåsa	0.39 ± 0.16	0.26 ± 0.12	0.27 ± 0.10	0.28 ± 0.10	0.30 ± 0.07
71550 Ørland	0.25 ± 0.07	0.21 ± 0.06	0.22 ± 0.06	0.21 ± 0.05	0.22 ± 0.04
75600 Leka	0.29 ± 0.12	0.28 ± 0.10	0.26 ± 0.11	0.24 ± 0.09	0.27 ± 0.06
77420 Majavatn	0.47 ± 0.20	0.33 ± 0.12	0.29 ± 0.11	0.30 ± 0.11	0.35 ± 0.08
80700 Glomfjord	0.44 ± 0.13	0.44 ± 0.09	0.38 ± 0.10	0.42 ± 0.12	0.42 ± 0.07
82290 Bodø	0.43 ± 0.13	0.42 ± 0.09	0.36 ± 0.09	0.40 ± 0.11	0.41 ± 0.07
85910 Røst	0.30 ± 0.09	0.30 ± 0.06	0.26 ± 0.07	0.28 ± 0.08	0.28 ± 0.05
89950 Dividalen	0.54 ± 0.16	0.40 ± 0.11	0.31 ± 0.12	0.41 ± 0.11	0.41 ± 0.07
90450 Tromsø	0.48 ± 0.14	0.42 ± 0.09	0.28 ± 0.07	0.36 ± 0.10	0.39 ± 0.06
92700 Loppa	0.45 ± 0.13	0.39 ± 0.08	0.26 ± 0.07	0.33 ± 0.09	0.36 ± 0.06
93300 Suolovuopmi	0.60 ± 0.18	0.41 ± 0.11	0.32 ± 0.13	0.43 ± 0.12	0.44 ± 0.07
93900 Sihccajävri	0.67 ± 0.20	0.43 ± 0.12	0.34 ± 0.13	0.47 ± 0.13	0.48 ± 0.08
96400 Sletnes	0.58 ± 0.11	0.44 ± 0.07	0.28 ± 0.11	0.44 ± 0.08	0.43 ± 0.05
97250 Karasjok	0.79 ± 0.23	0.44 ± 0.12	0.33 ± 0.13	0.48 ± 0.13	0.51 ± 0.08
98400 Makkaur	0.59 ± 0.12	0.45 ± 0.07	0.29 ± 0.11	0.46 ± 0.08	0.45 ± 0.06
98550 Vardø	0.58 ± 0.11	0.42 ± 0.06	0.27 ± 0.10	0.43 ± 0.07	0.42 ± 0.05
99710 Bjørnøya	0.83 ± 0.22	0.60 ± 0.15	0.39 ± 0.07	0.51 ± 0.13	0.58 ± 0.12
99720 Hopen	1.09 ± 0.29	0.51 ± 0.19	0.30 ± 0.09	0.67 ± 0.17	0.64 ± 0.14
99840 Svalbard Lufthavn	0.99 ± 0.27	0.52 ± 0.20	0.29 ± 0.09	0.62 ± 0.16	0.61 ± 0.14
99910 Ny-Ålesund	0.87 ± 0.23	0.47 ± 0.18	0.28 ± 0.08	0.58 ± 0.15	0.55 ± 0.12